AD-A097 697 ROYAL AIRCRAFT ESTABLISHMENT FARNBOROUGH (ENGLAND) F/G 14/2
MEASUREMENTS OF THE DYNAMIC PERFORMANCE OF THE MAIN DRIVE FAN O--ETC(U)
APR 80 R W JEFFERY
UNCLASSIFIED RAE-TR-80043 DRIC-BR-76275 NL

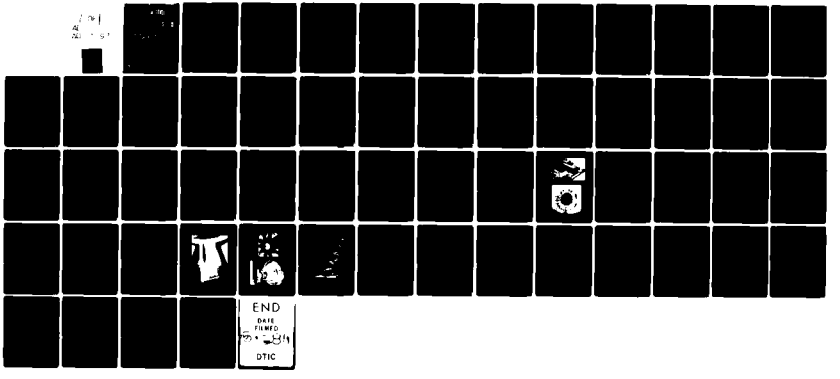

(9) Technical rept.,

LEVEL II (1)

ROYAL AIRCRAFT ESTABLISHMENT

(14) * RAE-TR-80043

Technical Report 80043

(11) April 1980

(12) 58

(6) MEASUREMENTS OF THE DYNAMIC PERFORMANCE OF THE MAIN DRIVE FAN OF THE RAE 5 METRE PRESSURISED LOW SPEED WIND TUNNEL.

by

(10) R.W. Jeffery

*

Procurement Executive, Ministry of Defence
Farnborough, Hants

REPORT DOCUMENTATION PAGE

Overall security classification of this page

UNCLASSIFIED

As far as possible this page should contain only unclassified information. If it is necessary to enter classified information, the box above must be marked to indicate the classification, e.g. Restricted, Confidential or Secret.

1. DRIC Reference (to be added by DRIC)	2. Originator's Reference	3. Agency Reference	4. Report Security Classification/Marking
	RAE TR 80043	N/A	UNCLASSIFIED

5. DRIC Code for Originator	6. Originator (Corporate Author) Name and Location
7673000W	Royal Aircraft Establishment, Farnborough, Hants, UK
5a. Sponsoring Agency's Code	6a. Sponsoring Agency (Contract Authority) Name and Location
N/A	N/A

7. Title Measurements of the dynamic performance of the main drive fan of the RAE 5m pressurised low speed wind tunnel

7a. (For Translations) Title in Foreign Language

7b. (For Conference Papers) Title, Place and Date of Conference

AIAA 11th Aerodynamic Testing Conference, Colorado Springs, 18-20 March 1980

8. Author 1. Surname, Initials	9a. Author 2	9b. Authors 3, 4	10. Date	Pages	Refs.
Jeffery R.W.			April 1980	56	9

11. Contract Number	12. Period	13. Project	14. Other Reference Nos.
N/A	N/A		Aero 3478

15. Distribution statement

(a) Controlled by – DRPC via DRIC

(b) Special limitations (if any) –

16. Descriptors (Keywords) (Descriptors marked * are selected from TEST)

Wind Tunnel. Main Fan. Dynamic Performance.

17. Abstract

Tests were carried out to monitor and evaluate the performance of the blades in the main drive fan of the 5m pressurised low speed wind tunnel. A technique was developed for *in situ* maintenance checking to detect the onset of internal cracking or delaminarisation in the glass reinforced plastic blades. Three of the ten fan blades were instrumented with strain gauges to monitor the dynamic performance of the fan under different loadings resulting from combinations of fan speed and tunnel pressurisation. The effect of a model was also investigated, with the model both stalled and unstalled.

F5910/1

UDC 533.6.071 : 533.6.011.32/34 : 533.6.071.1 : 533.662.3

ROYAL AIRCRAFT ESTABLISHMENT

Technical Report 80043

Received for printing 14 April 1980

MEASUREMENTS OF THE DYNAMIC PERFORMANCE OF THE MAIN DRIVE FAN OF THE RAE 5m PRESSURISED LOW SPEED WIND TUNNEL

by

R. W. Jeffery

SUMMARY

Tests were carried out to monitor and evaluate the performance of the blades in the main drive fan of the 5m pressurised low speed wind tunnel. A technique was developed for *in situ* maintenance checking to detect the onset of internal cracking or delaminarisation in the glass reinforced plastic blades. Three of the ten fan blades were instrumented with strain gauges to monitor the dynamic performance of the fan under different loadings resulting from combinations of fan speed and tunnel pressurisation. The effect of a model was also investigated, with the model both stalled and unstalled.

Departmental Reference: Aero 3478

LIST OF CONTENTS

1 INTRODUCTION

The RAE 5m pressurised low speed wind tunnel has been in operation at Farnborough since December 1977[1]. Fig 1 shows an aerial view of the facility taken at the time of commissioning. It was built to improve accuracy and reliability in wind tunnel tests of the low speed aerodynamics of aircraft, complete with their high-lift systems. High unit Reynolds numbers are achieved by using a large test section, by working at total pressures up to 3 atmospheres and by having large installed power for fan main drive. Independent control of tunnel pressure allows a 3:1 range of Reynolds number at constant Mach number and allows the effects of scale and compressibility to be separated. This gives a firm base from which to extrapolate to full-scale values. Models of small combat aircraft can be tested at full-scale values of Reynolds number, while models of large transport aircraft can achieve about one quarter of the flight value.

The tunnel fan is located in the return leg of the tunnel circuit, the drive motors (11 mW ac and 1.64 mW dc) being housed in a nacelle of 6.1m diameter in the air passage. The fan has 10 blades of fixed pitch and airspeed variation and control is obtained by changing the rotational speed of the motors. Fig 2 shows a general view of the fan and nacelle assembly.

The purpose of this Report is to record some of the detail of the design, manufacture and testing of the fan blades and then to describe the in-service performance. Much more detail of the fan assembly, the motors and their control system is contained in the manuals for the tunnel, but sufficient detail is included here for completeness. The in-service performance is dealt with in two parts. The first part covers the development of a 'wheel-tapping' technique for the maintenance checking of the fan blades and details the results so far. The second summarises the dynamic performance of the fan assembly through a range of tunnel pressures and speeds and also demonstrates the effects on the fan due to a model both at normal incidence and beyond the stall.

2 DESIGN OF THE FAN BLADES AND THE HUB ASSEMBLY

The main drive unit is made up of a nacelle, containing the two drive motors and the support for the fan and main drive shaft, together with a nose cone carried on 21 cambered and twisted pre-rotation vanes. The nacelle is supported on nine straightener vanes in the return leg and three of the vanes admit or discharge air to and from the tunnel through slots in their trailing edges. The fan and motor assembly is supported by a single stiff bed-plate forming part of the internal structure of the nacelle, downstream of the fan. The fan itself is

supported from a hollow pedestal by a spherical roller bearing and is driven from the upstream side by a shaft which passes back through the pedestal. This arrangement gives a stiff mounting for the fan and allows either the fan bearing or the shaft to be removed, while the fan is left *in situ*.

The fan has an outside diameter of 10.0 m and each blade is 1.885m long with a constant chord of 0.900 m. The thickness to chord ratio varies from 10% at the tip to 20% at the root. Each blade is a fibreglass structure with both camber and twist and is basically a multi-spar hollow structure with a thick skin which is bonded to an aluminium alloy root fitting carried on a welded steel spoked hub. Each spoke is a welded steel box bolted between two side plates which are fixed to a cast steel centre to form the hub. The blades were made from glass reinforced plastic; wood and light alloy construction being discounted. The main reasons for GRP were the relatively high specific strength, the accuracy between blades, localised damage and subsequent ease of repair and the existence, at RAE Bedford, of an experienced workshop department. Light alloy was rejected because of cost, difficulty of repair and susceptibility to fatigue. Wood was rejected through concern over stability, especially in the changing pressure environment and dry conditions in the tunnel, weight consistency and worries over labour shortage. Because of these concerns, design for timber blades was not taken sufficiently far as to ensure structural acceptability.

The aerodynamic design of the blades was based on the results of Ref 2. The calculations were made for one particular tunnel condition; a working section speed of 107 m/s and a stagnation pressure of 2.2 atmospheres. This condition corresponds to the maximum power and Reynolds number and additional checks were made to confirm a satisfactory performance over the full operating range of the tunnel.

After the initial design calculations, tests were made to help in defining the geometry of the passage approaching the fan and to check on the performance of the pre-rotation vanes[3]. The fan is positioned a short distance downstream of the second corner at a point where the tunnel diameter is moderate, limiting the size and the cost of the fan unit and giving a relatively high air speed and good fan efficiency for sensible rotation speeds. The speed is not so high that problems of noise or compressibility become important (the tip speed is limited to M ~0.46). For mechanical simplicity the blades have a fixed pitch and the fan and nacelle diameters were set by the requirement to provide a nearly constant area of duct through this section of tunnel, with the size of the nacelle fixed by the dimensions of the main drive motors. The blade lift coefficients were kept

low so as to avoid any possibility of stalling with a high drag model in the tunnel. More detail of the design and manufacture of the fan blades is contained in an Appendix at the end of this Report.

3 MAINTENANCE CHECKING OF THE FAN BLADES

During manufacture and before the first tunnel run, the 15 individual blades were evaluated in a series of static and dynamic tests as a check on manufacturing consistency before assembling 10 of them into the fan. As a part of this testing, one additional blade was subjected to a distributed load, representing the combination of aerodynamic and centrifugal forces, through loading points bonded in the top and bottom surface. In that test, reported in the Appendix, blade deflections were measured at 12 points and strain was measured on the flange which supports the blade on its steel spoke. In a second test series, of dynamic measurements, resonant frequencies and modal shapes were identified for fundamental and high order bending and torsion modes for each of the manufactured blades. These tests also demonstrated a consistency of manufacture over all of the blades.

For these resonance tests, carried out by Structures Department[4]; each blade was bolted to a heavy bed-plate using the integral root fitting. The blade was mounted vertically and the tests made using the MAMA equipment[5]. Two electromagnetic exciters were slung on wires from an overhead framework and attached to the blade, at two points near to the blade tip, by push-rods connected to screw fittings bonded to the blade surface. The excitation forces were applied normal to the centre line at the tip.

Blade response was measured by three accelerometers, two of which were mounted at the excitation points but on the opposite surface to the exciter push-rods. The third accelerometer was mounted on a suction-cup device and could be attached to the blade at any point. For each mode this accelerometer was applied at 36 positions spaced over the blade, in order to determine the mode shape. The damping value was found from a vector plot for which the excitation was that appropriate to pure mode excitation. For subsequent blades, once the mode shapes were established, only the frequency and damping for each mode were measured. Fig 3 shows the results for frequency, percentage critical damping and basic mode shape for the 15 blades. Highlights of the results are as follows:

(i) Modes 5 and 7 correspond to chordwise bending modes and their comparatively low frequency is attributed to the absence of any rib structure.

(ii) The nodal line in mode 3 shows that the blade is far stiffer in bending at the root than at the tip.

These results demonstrated a very good consistency in manufacture and identified the nine basic modes of vibration. For the routine maintenance checks on blades in service, this technique was extended to monitor the frequency of selected modes in order to detect the onset of delaminarisation in the glass-fibre, or an incipient failure in the internal structure or bonding to the root fitting. Each blade was fitted with hard points near the leading and trailing edges, corresponding to the position of the exciters in the dynamic tests and seen in Fig 10. Accelerometers are fixed to these points and signals from them are recorded for a series of hits with a rubber hammer at both leading and trailing edges. The data, for each blade, is analysed using an FFT computer technique suggested by Copley in Structures Department[6].

Figs 4 and 5 show typical spectra from one particular blade. In Fig 4 the blade was hit at the trailing edge and the response of the two accelerometers is shown; Fig 5 shows the response to a leading edge strike. All of the modes seen in the static testing, with individual blades mounted on a heavy bedplate, can be seen in the accelerometer results for each blade when assembled into the complete fan. The 100 Hz bending mode is not pronounced and the 250 and 330 Hz modes are only seen on some of the traces. In comparison with Fig 3, differences may be due to mounting the blades onto the steel hub and the behaviour of the complete assembly. The modes at 75 Hz and at 330 Hz now show complicated double peaks on some traces and this could be another effect due to the complete structure rather than an isolated blade.

To monitor the integrity of each blade, the spectrum resulting from a series of strikes is subjected to a detailed frequency analysis using RAE Structures Department PAPA techniques[7]. From the nine basic modes, three are chosen as being clearly defined; the modes at 23, 75 and 150 Hz. The frequency and damping for each of these chosen modes are accurately measured and the independent results from the two accelerometers used to confirm the result. In general the agreement between the two sensors, at opposite ends of the chord, is 0.01 Hz or better. Generally, strikes at either leading or trailing edge have provided sufficient data but the second set can be used to resolve differences between the two accelerometers. While the agreement in frequency is very good, the results for damping are more variable. The maintenance checking is therefore based on the measured frequency in the chosen mode for each blade, the data providing four measurements of frequency for each blade at each of these different mode frequencies.

These 'wheel-tapping' checks have continued since the first tunnel runs in December 1977. Initially, the blades were checked after each excursion to a new and higher power level, up to the maximum continuous rating. While the fan was still relatively new the checks were performed at regular intervals, but the 'wheel-tap' is now written into the maintenance schedules to be carried out after every 100 hours of tunnel running.

Results are therefore available for a range of ambient temperatures and Fig 6 shows the variation in the first flapping mode measured on Blade 8 over the temperature range from 0 to 26°C. The temperature is that of the blade surface, measured using a thermocouple in contact with the material of the blade. The results show a decreasing frequency with blade temperature and so demonstrate a marked change from day-to-day. This same variation will lead to a gradual change in blade response even during a tunnel run, as the blade temperature rises or falls with demanded air temperature.

The method used for the long term monitoring must take account of this day-to-day variation. The measured frequency, in a given mode, for each blade is therefore normalised by the averaged frequency for the complete set of blades, all measured during the same test:

$$R_x = f_x \Big/ 0.1 \sum_{z=1}^{10} f_z$$

where x is the blade in question. The results are shown, in this form, in Figs 7 and 8 for the three modes used in the analysis. Fig 7 also shows selected data for the measured percentage critical damping for the set of 10 blades. The damping measurements from the leading and trailing edge transducers are seen to be inconsistent but roughly in agreement with results from the static tests. The changes due to temperature are reflected in the variations of average frequency for each of the modes. As well as the average frequency and the normalised value for each blade, shown in Fig 7 for the first flap mode, Fig 8 gives the summarised results to date. The average of the normalised frequency over all of the checks so far, together with the standard deviation of the result, is shown. Variations in average temperature are large, indicating the change from day-to-day, but the variation in normalised frequency is small. This parameter is seen to correlate the results so far and should provide a clear indication of any breakdown in a particular blade, which would cause a marked change in frequency.

043

From these results, one of the chosen modes (first order torsion at 75 Hz) is seen to give relatively poor results. Examination of Figs 4 and 5 confirms a complicated response in that particular mode and further tests did show two closely spaced vibration modes; typically at 69 and 75 Hz. In the long term, it may therefore be better to base the analysis on just the 23 and 150 Hz modes. On one occasion the tip of Blade 14 was damaged when a plywood panel lifted and was blown round the circuit. The blade was removed for repair and replaced by Blade 10, which explains the one occurrence in Fig 7 for Blade 10.

Of course, to establish the technique fully, a test specimen, and preferably a complete blade, should be tested in various states of failure so that the effect of progressive internal breakdown can be known. So far this test has not been planned and there is no clear idea of what the effect of a crack might be. However, the blades have so far behaved in a normal way and, for the first 600 h of tunnel running up to August 1979 at least, no significant variations have been seen. The maintenance checking, based on this technique, will therefore continue to be used as the method to monitor the life of the fan blades in service. Hopefully, the experience of the Arnold Engineering Development Centre with the Propulsion Wind Tunnel Facility is an indication of the success of fibreglass plastic blades. After the failure of steel compressor blades at the point of attachment to the compressor disc, they were replaced by plastic blades. The facility has subsequently run for many thousands of hours without need for any more than local patching after foreign object damage[8].

4 DYNAMIC PERFORMANCE OF THE FAN

To monitor the performance of the fan in use, three of the ten fan blades have been instrumented with strain gauges, arranged as complementary full bridges with two gauges on the top surface and two on the bottom. Each of the three blades has five gauge positions, arranged to be sensitive to the three basic modes of vibration; flapping, torsion and chordwise bending. The actual positions for the gauges were established through tests with one of the spare blades using the same experimental technique as was used to evaluate the blades after manufacture. The spare blade was bolted to the heavy bed plate and each of the nine vibration modes excited in turn using the MAMA equipment[5]. Blade response was measured by three displacement sensors and two accelerometers. The gauge positions were optimised so that the nine vibration modes were properly seen by the set of five bridges, each bridge being more sensitive to either flapping, torsion or chordwise bending. Fig 9 shows the positions chosen and also indicates which gauges were found to be sensitive to particular vibration modes. The

Figure is in two parts. The top part shows the position and orientation for each gauge position; based on the orientation of the gauges the likely sensitive response is indicated. The bottom part shows the results of the tests, as the recorded voltage for each gauge position with the same gain setting and amplitude of excitation. Also shown is the response for each gauge position, normalised by the maximum response for that gauge in one of the nine modes. (This gives an indication of the most sensitive mode for each gauge position.) The results show that although position 3 was designed to be sensitive to torsion, by the orientation of the individual gauge elements, the response was in fact predominantly in the first order flapping mode. For position 1, supposedly optimised for flapping modes, there was a significant response in the torsion modes and position 5 was the best position for all of the higher-frequency modes, not only chordwise bending.

Considerable thought was given to the problem of taking signals away from the bridges on the rotating fan blades. A particular worry was the close proximity of the very large (11.00 mW) ac motor and the controlling dc motor (1.64 mW). Radio transmitters, with amplifiers and transmitters mounted on the hub were considered as was a system based on some sort of magnetic pick-up between the rotating shaft and the fixed tunnel structure. Eventually it was decided that a system based on good quality instrumentation slip rings mounted on the upstream side of the hub gave the best solution. The massive steel hub structure would shield the slip ring from the magnetic influence of the motors but careful screening would be necessary for the wiring on the blades. Most of the chosen bridge positions were close to the blade root but one position, particularly sensitive to the chordwise bending modes, was close to the blade tip and required a considerable length of signal wire. All of the instrumentation cables were screened in 'μ-metal'. The positions close to the root were under the root-fixing fairings so the screened wires were run on, and bonded to, the surface of the blade. For the top and bottom gauges of the tip position the wiring was recessed in a channel cut parallel to the tip and then down the trailing edge of the blade. The wires were wrapped in 'μ-metal' and the surface made good to present no aerodynamic disturbance. Fig 10 shows a typical instrumented blade, with the tip position and the filled wiring trench clearly visible. The root gauges are contained below the fairings seen at the top of the photograph. The hard-point fixings for the wheel-tapping accelerometers can also be seen at leading and trailing edges.

043

The signal wires were terminated at a connector mounted on the root fixing of each of the three instrumented blades. These three were adjacent blades. The signals were taken across the hub/spoke assembly, through fully screered cables,

to the slip ring, as shown in Fig 11. Because of the number of channels involved, the large (24-way) and heavy slip ring unit was mounted in reverse; the body of the slip-ring being carried on the hub-mounted plate fixed to the front of the main drive shaft and the small rotating shaft held stationary by a support fixed to the tunnel structure. The plate also carried balance circuits for each of the 15 bridges and amplifiers so that the signals were amplified before passing across the slip ring and away from the rotating fan. Both the balance circuits and the amplifiers were housed in 'μ-metal' cases carried on the top surface of the hub plate and also shown in Fig 11.

The amplifier, the power supply and the bridge balance circuits were copies of those used in model tests to measure the vibration mode shapes of a rotating helicopter blade[9]. The signals were taken from the slip ring on the fan to a set of line-drivers and from there to the Observation Room along well-screened analogue cables.

The signals were analysed using a Digital Signal Analyser over the frequency range from 0 to 400 Hz. Based on the evaluation summarised in Fig 9, and because of the limited time available, the dynamic performance of the fan was assessed by measurements at gauge positions 1 and 3 on Blade 11. These positions, in combination, were reasonably sensitive to the various basic modes (and not all of the 15 channels were operating). Also, the signal level from these two positions was adequate and the signals themselves free from any interference. Fig 12 shows typical spectra for both gauge positions for a representative tunnel condition, with fan rotation speed of 226 rev/min and pressure level of 300 kPa. The plot is presented as a high-resolution auto-spectrum, the magnitude being presented on a dB scale relative to 1.0 V. Both gauge positions demonstrate basically the same response, but position 3 is more sensitive to the modes at 100 and 200 Hz as well as showing the other modes seen at position 1. Both positions, 1 and 3, were sensitive to flapping by the orientation of their elements. The major response from position 3 is in the basic flapping mode, which shows a response some 7 dB above the response in the torsion mode, for this particular tunnel condition. For position 1, however, the response in the torsion mode is some 12 dB greater than the response to flapping, but the level of signal is in general some 20 dB less than the other gauge position. This is confirmed by Fig 9; the response to flapping is five times greater at position 3 than it is at position 1. This is for identical gain on the two channels, whereas in the measurements from the fan in use the gain settings on each channel are different and, for the tunnel tests, the response is some 10 times greater at position 3.

In Fig 12 the first nine modes, except for that at 303 Hz, are all seen clearly in the spectra for the two positions. In addition, very clear harmonics of the basic rotation speed are present (and this proved a useful check with the indicated fan speed from the motor control system). The response of the individual blade, through a range of rotation speed and tunnel pressurisation, is assessed by integrating the area beneath the frequency spectrum, for each gauge, over a frequency range from 15 to 375 Hz. The lower limit is set to avoid the rotation speed harmonics and the upper to limit the analysis to the first nine modes. Fig 12 shows these boundaries; between the two limits the area under the curve is taken as a measure of the power contained in the vibrating modes (and the Figure would be repeated for each speed and pressure combination to give the dynamic response in terms of vibrating power).

Fig 13 shows the output for the two gauge positions as the blade is moved through one complete revolution. The blades are inclined forward and, as the fan rotates, the weight of the blade is transferred into the root fixing through the upper and lower skins of the open box structure. Since the amplifier gain settings are the same as were used for the dynamic measurements, this can be thought of as a calibration of the two gauge positions, as the physical dimensions and weight distribution of the blade are accurately known. The results show that the signal from gauge 3 is about 20 dB greater than that from the second position, gauge 1.

Fig 14 shows the interference diagram in which the blade frequencies, for the basic modes, are shown cross-plotted against rotation speed - there being a centrifugal effect which increases the mode frequency with increased rotational speed. The likely sources of fan-ordered excitations are shown on the diagram. Twenty-first order excitation results from each blade passing through the wakes of 21 pre-rotation vanes and is the most likely source of aerodynamic excitation. The predicted resonant conditions are fan rotation speeds of about 65, 200, 220 and 300 rev/min (depending on blade temperatures and the exact centrifugal effects). Also shown is a motor frequency at 34.8 Hz. This is a shaft vibration where the dc motor oscillates on its shaft, which connects to the ac motor shaft. However, a Holset coupling effectively isolates the fan shaft from the motors, except at about 7 Hz, and so the aerodynamic excitation which would coincide at about 100 rev/min should not lead to any motor instabilities, which could be felt at the blades. Excitations of 10 fan orders and 210 fan orders might also be felt by the shaft, but again should be isolated from the blades.

Fig 15 shows the detailed dynamic performance at atmospheric pressure as measured at the two gauge positions, 1 and 3. Each point on the graphs represents the result of the integration between frequency limits to obtain a measure of the power contained in the vibrating modes at a particular fan speed. The peaks therefore correspond to different modes being excited at particular fan speeds through the operating range, rather than a single mode in resonance at different rotation speeds. As was found in the test to optimise gauge positions, although position 3 was orientated to be sensitive to torsion, its major response was to the first order flapping mode and position 1 was sensitive to both flapping and torsion modes and therefore demonstrates more resonance peaks through the speed range. The results show that at some fan speeds either torsion or flapping modes are excited; for example at 64, 80, 176, 211 and 300 rev/min the flapping modes are excited (since gauge 3 responds), at 201 rev/min the torsion modes and at 112 rev/min both modes respond.

Based on these selected fan speeds, each of which corresponds to a resonant condition in one or more of the basic modes of vibration, Fig 16 is an attempt to identify the particular mode which is excited at each of the resonant conditions, marked on Fig 15. At these selected fan speeds, in addition to integrating the signal over the frequency range to have a measure of vibrating power, the amplitude of each peak (each corresponding to one of the basic modes) was recorded from a detailed spectrum for the first four basic modes. The amplitudes of the peaks in the first four modes were plotted against fan rotation speed for each gauge position. Of course, not all four modes were seen by both gauges so, of the eight possible curves in Fig 16, only six are present. Where the same mode is seen by both gauges, first flap and first torsion (and at torsion resonance, despite earlier comments about gauge 3, the response was clearly seen by both gauges - see Fig 17) - the response of the two gauges was very much the same. The two second order modes are each seen by only one of the two gauges, again shown in Fig 17. Because the detailed spectra were only recorded at selected fan speeds, the data has been normalised to the lowest speed, 64 rev/min which corresponds to first order flap excitation. The data has also been adjusted for different sensitivity and gain settings for the different gauges. Also shown on Fig 16 is a theoretical curve corresponding to a doubling of power for a doubling of air speed or fan rotation speed. (This theoretical curve is also shown in Fig 15.)

Several conclusions can be drawn; the torsion modes and the second flapping mode respond as expected to increased dynamic pressure. The basic flapping mode

is complicated at the low speed conditions, and is in fact increasing, because this is where the blade passing frequency is able to excite that mode. The increases at higher fan speeds are much as expected for increased dynamic pressure and the increase at about 64 rev/min is the expected resonance for a blade passing behind 21 pre-rotation vanes with a mode frequency of about 23 Hz (depending on temperature). For the next two modes, basic torsion and second order flap, excitation would be expected at fan speeds of 200 and 300 rev/min (with a possible event at 220 rev/min corresponding to the double peak seen in the static tests for the torsion mode).

These fan speeds have been marked on Fig 16. Since all of the selected spectra have been normalised to the 64 rev/min, first-flap condition, this resonance can only really be seen by reference to Fig 15, and in particular gauge position 3 which is more sensitive to flapping modes. However, at about 205 rev/min a clear increase is seen for the first torsion mode (with allowance on the actual speed for temperature and centrifugal effects). At 300 rev/min there is an increase in the second flap mode but for the second torsion mode, with a frequency of about 160 Hz, the excitation speed is outside the maximum fan speed and no definite resonance is seen for this mode. In all of the tests, to measure fan dynamic performance, the tunnel was running so that the fan rev/min was set manually and the air temperature was automatically controlled to a set temperature of 20°C, so that the temperature environment for the blades was nearly constant.

Fig 17 is a collection of the individual spectra for the two gauge positions for each of the selected fan rotation speeds. The effects of resonance in a particular mode, summarised in Fig 16, can be clearly seen by an increase at the mode frequency at resonance. (However, the vertical scale is not constant and should be considered when reviewing the basic data shown in Fig 17.)

Many of the resonant or driven conditions seen in Figs 15 and 16 are also seen in the interference diagram of Fig 14. In particular, the intersection of the twenty-first fan order with the first three basic modes, at approximately 65, 200, 220 and 300 rev/min, corresponds with peaks in the dynamic performance. All of these fan speeds are conditions where dynamic activity is increased; the region around 215 rev/min is an area of confusion, with several closely-spaced excitations shown especially by the torsion-sensitive gauge. In general the peaks seen in the dynamic performance can be explained by pre-rotation vanes providing a driving input at the appropriate frequency to excite the basic fan modes

and the motor shaft oscillation. However, there are still some modes for which the excitation cannot be identified in terms of the pre-rotation vanes.

Figs 18 and 19 show the effect of tunnel pressurisation on the fan blades, as measured at the two different gauge positions. Results are shown for 100, 200 and 300 kPa total pressure, which, based on the increase of aerodynamic load, should cause an increase of 6.0 and 9.5 dB respectively. Although the general level of response is increased, that increase is more like 5 and 8 dB, not quite up to the theoretical value. The modes at low frequency (low rotation speed) are increased in their response, but at higher rotation speeds the modes are much reduced, presumably due to increased aerodynamic damping. In particular, the mode seen at 100 rev/min on gauge position 1 is pronounced at higher pressures. The results for gauge position 3 (dominated by the flapping response) shows a large increase in the first order flapping response with increased tunnel pressure. This increase approaches the predicted 9 dB for tunnel pressures of 300 kPa. The results for higher fan speeds show that the flapping modes are more damped at increased pressure than were the results for the other gauge position. Since gauge 1 is more sensitive to torsion this indicates that the increased aerodynamic damping is more effective in flapping than in torsion.

Figs 20 and 21 show the effects due to the presence of a model in the test section, again for the two different gauge positions. All previous results were for an empty tunnel. For position 1 (torsion and flapping), the only effects of a model, both stalled and unstalled, were in the fan speed range between 175 and 225 rev/min. This has been seen to be a complicated region in terms of fan dynamic response and so the presence of a model is beneficial, but there is very little difference between a stalled and unstalled model. For the 'flapping' gauge, position 3 Fig 21, the unstalled model causes a decrease of activity between about 175 and 200 rev/min but increases the resonance at 215 rev/min, believed to be associated with first mode torsion. However, the stalled model damps the response above 200 rev/min as well as between 175 and 200 rev/min. In all cases the wake of the model, in this case a 1/13 scale A300B, appears to break up a regular flow at fan speeds around 200 rev/min and does not introduce any other excitations in doing so.

5 CONCLUSIONS

The Report has dealt with the results of tests performed on the blades of the main drive fan of the 5m pressurised low speed wind tunnel during commissioning of the new facility.

A technique is described for the routine maintenance checking of each fan blade to test for the onset of internal cracking or delaminarisation. The results are so consistent that incipient damage will show up as a marked change in the frequency of one or more of the basic modes of vibration. Ideally a test should be made on a test piece, through a range of simulated damage, to establish exactly what these changes might be.

Three of the 10 fan blades have been instrumented with strain gauges in order to monitor the dynamic performance of the fan under different loading conditions both with and without a model in the working section. Resonant conditions were seen but their level is less than the levels of non-resonant conditions at maximum fan speed. Generally these excitations can be explained in terms of blades passing behind the 21 pre-rotation vanes. The presence of a model is beneficial but the effect of increased pressure is to increase the level of response. However, the increased aerodynamic loading appears to introduce extra damping and the resonant conditions are suppressed at higher tunnel pressures.

Acknowledgment

The measurements were made on the complete main drive fan of the 5m tunnel which was designed and manufactured by Royal Aircraft Establishment personnel. Obviously, all credit is due to the designers and craftsmen responsible for that work and the only purpose of this Report is to record the results of some tests carried out during the commissioning and early running of the tunnel. In this I should like to record my thanks to those in Structures Department RAE who assisted, in many ways, with the instrumenting of the blades and the analysis of the data; particularly noteworthy was the help given by the late Chris Hassal.

Appendix

MAIN DRIVE FAN DATA MANUAL

A.1 Fan blade

A.1.1 Design philosophy

Materials considered for manufacture of the blades were light alloy, wood and glass reinforced plastic. GRP was finally selected because of its relatively high specific strength, inherent self damping qualities and apparent economy in manufacture for the number required. Influencing this decision were also the following points:

(i) Light alloy was rejected on account of its probable cost and it was considered less easy to repair in the event of damage and more prone to fatigue.

(ii) There was doubt concerning the stability of wood under the changing working pressure and dryness to be experienced in the tunnel. Difficulty would probably be experienced in obtaining timber of suitable quality, either in mahogany, Sitka spruce or Douglas fir.

There were recollections in the Woodwork Shop of manufacture of spare blades for the 24ft tunnel and labour shortages foreseen, whereas, there was in existence in the RAE Bedford Workshop, an experienced section thought well able to undertake manufacture in GRP. Other advantages thought to be gained from using GRP were that each blade would be dimensionally identical externally, being manufactured in the same moulds, which would exist for subsequent manufacture of spare blades. In the event of striking a foreign body during running, damage would tend to be localised or lend itself to repair *in situ*.

Having selected GRP there must inevitably be compromise in the design to suit conflicting requirements in loadings and to suit the methods of manufacture thought most likely to be satisfactory in practice, bearing in mind the Workshop technique already known and proven by the staff concerned. Investigations showed that other blades known to have been made in GRP (eg Messerschmitt-Bolkow-Blohm Helicopter, Rotol Hovercraft, Dama Plastics (USA) Helicopter) had used a fairly thin GRP skin with a unidirectional glass fibre spar and with the blade interior filled with foamed plastic to stiffen the skins. As no satisfactory evidence concerning the long term stability of foamed plastic under the anticipated operating condition could be established, this method of construction was rejected. The design selected was a multi-cellular construction with comparatively thick

skins. The skins were to be hand-layered in two parts (upper and lower), in moulds, using techniques already known in the Workshops. The two skins were then to be joined by bonding at the LE and TE and at each of the web/skin junctions.

The main disadvantage with hand-layered GRP composites is in maintaining a satisfactory glass/resin proportion and in maintaining consistency. The alternative would be to use pre-impregnated material with a thermo-setting resin or similar process, possibly bag moulding or using matched dies. These methods had not been used to any appreciable extent in the RAE Workshops, particularly for such large components, whereas over a number of years tests and checks had been made on hand-layered epoxy/glass composites for use on experimental equipment on aircraft, and acceptably consistent results had been obtained for strength and glass/resin ratio. Thus it seemed reasonable that if substantially the same team of skilled men could be used throughout, no great difficulties would be met as regards composite consistency, and the lower strengths and rigidity to be obtained could be allowed for in design.

A.1.2 Functional description

The resin selected (after consultation with CIBA) is Araldite CY219 (MY750) 100 pbw; Hardener CY219 50 pbw; Accelerator DY219 1 pbw. This is a general purpose laminating resin of good mechanical strength. After room temperature cure for 3 days, post curing for 4 h at 100°C gives maximum operating temperature 75 to 80°C which gives ample factor over the anticipated tunnel ambient temperature of 45°C.

The main loads to be withstood by the skins are tensile loads caused by centrifugal forces and air loading, chordwise bending loads caused by air loading and torsional loading due to aerodynamic and centrifugal forces. Torsional stiffness is of importance, it being required that twist under load should be within a maximum of 0.25°. To meet these requirements a substantially isotropic reinforcement system is required and a balanced lay-up 2 x 0°, 1 x 45°, 2 x 0°, 1 x -45°, 2 x 0° etc was selected, using 8 shaft satin glass cloth to BS 3396/3/S2/225E. Tests for fatigue on laminates using this material are well documented, particularly from American sources for 181 cloth to Mil C9084, which is the American equivalent material.

Mechanical tests on the composite, as produced in the Workshop under production conditions, gave ultimate tensile strengths in the range 32000 to 34000 lb/sq in, values for the elastic modulus in tension as 1.60×10^6 and modulus in shear 0.90×10^6.

043

Based on these strength tests a working stress of 3000 lb/sq in was selected for design, any dynamic stress being superimposed. This working stress is sufficiently low to take into account the fatigue strength of the composite, any off design condition of fan running, together with a defect factor for improper workmanship, faulty material or processing. It is in line with the requirements for pressure vessels manufactured in similar materials for which a factor of 10 is required in the short term test strength of the material.

As a basis for comparison, the weight of active blade section is estimated at 192 lb, as compared with 175 lb Sitka spruce and 275 lb mahogany. It is probable, however, that the root attachment would be heavier for the wooden blade than for GRP.

For a given air pressure, fan blades could be 'coned' so as to give zero root bending moment by balancing the effects of centrifugal and thrust forces. Because the 5m tunnel works over the pressure range from 1 to 3 bar, the coning angle has been set to minimise the stresses; this gives the same maximum tensile stress on the upper surface at 1 bar and on the lower surface at 3 bar. Blade deflection markedly affects the moment of the centrifugal force, whilst scarcely changing the thrust moment and therefore causes a reduction in the resultant stresses.

For attachment of the blade to the hub structure, consideration was given either to utilise bolts or pins in shear via a suitable metal fitting attached to the fibreglass, or to use bolts in tension via a suitable metal flange connected to the fibreglass. The latter method was selected to facilitate assembly between the tunnel outer shell and the nacelle. With this method, by suitably pre-tensioning the bolts, the effect of any fluctuating loads would be greatly diminished and, with suitable load levels, the bolt fatigue life virtually infinite.

The general aerofoil shape of the blade has been extended inwards from the active portion to form the shape of the root flange. By suitable shaping of the root flanges the direction of the fibres is kept in line with that of the main axial forces. The root flange is an aluminium alloy angle around which the fibreglass is wrapped and bonded and is tapered in thickness to match as far as can be anticipated, the strains of the two materials.

At each bolt position a metal insert is set through the fibreglass to locate in the flange and in a base plate which is bonded to the fibreglass. The total bonded length, including the baseplate, is approximately 12 in. The shear stress of the bond has been tested to give minimum value of 1950 lb/sq ft giving

approximately 23000 lb/in of root flange length. The maximum load per in of root flange, resulting from centrifugal force and air bending moment is calculated to be 20,'8 lb (at approximately 10% chord on lower surface) to slightly better the required factor of 10 on stress.

In addition, the design of the inserts, which serve to provide metal spacers for the attachment bolts, is such that on failure of the bond with the root flange, the fibreglass must be pulled through the tapering gap between the inserts. With equal forces being applied to each side of the insert, there would be virtually no shearing force applied to the bolt, and, as the area of fibreglass between the inserts is equal to that of the skin at the root, there is an additional reserve factor of the same magnitude which would apply in the unforeseen event of failure of the root flange bond.

The bolts between the root angles are to prevent peeling action on the bonded joint and to resist bending action round the heel of the angle.

Tests on a section approximating to one cell portion of the blade showed adequate strength, although the full factor of 10 is not possible in a test section unless the metal portions such as tie bolts etc are strengthened to an equivalent factor. The test, however, did illustrate the effect of the inserts, as the final break of the fibreglass did occur between inserts after failure of the tie bolts and of the bonding of the root flanges. With several adverse conditions the test specimen failed at a load of 11500 lb/in of flange length (factor of 5 on the worst loaded position) but after consideration of the test condition it was decided that further testing was not necessary since failure of the metal components occurs at this factor.

The interior of the blade is vented to tunnel pressure via a hole in the hub spoke attachment flange. The blade tip is sealed by a balsa portion of effective spanwise length 3 in which can also act as a frangible tip to minimise damage in the event of a blade striking any object accidentally becoming loose in the tunnel.

Selection of the skin thickness has been made as a compromise between the requirements for bending forces, centrifugal forces, flexural torsional and spanwise rigidity together with requirements for manufacture in order to maintain accurately the aerodynamic form.

A.1.3 Calculations

For the purpose of design calculations the blade was considered divided into sections at the same radii as specified in the air loading data. For convenience in calculation all changes in skin thickness have also been made at these radii. Since the resultant force of the axial and circumferential aerodynamic loads is normal to the effective neutral axis of the blade throughout the span, the calculations for bending stress and positioning of the blade segment CG's have been made assuming the blade to be an untwisted cantilever. Subsequent to these calculated section positions, the blade was then faired to give acceptable lines of leading and trailing edges.

In order to facilitate blade mould and jig manufacture, all manufacturing dimensions are related to XYZ axes with X axis being at 19.18° to plane of rotation ie with blade rotated so that Station 4 is horizontal.

On completion of the blade design, a further set of calculations was made as a check and to provide loading data for a strength test to be made on the blade. This method comprised dividing the blade into small elements of area at each of the spanwise sections, the data being taken from the manufacturing information. These areas, together with their respective distances from the rotational plane were computed. The forces acting on these elements were then computed independently by the 5m tunnel development section at RAE Bedford and the total loads, together with points and directions of action, were obtained for the three design running conditions. The results of these calculations were in very close agreement with the original design figures.

Based on the 'area-element' derived load figures, one blade and spoke were tested to simulate the 2.2 atmosphere 310 rev/min, ie worst load condition. Tests were carried out to a maximum factor of 2.40, (this being the maximum possible due to machine limitations) without damage to blade or spoke. The blade used for this test was not one of the production batch, but rather a prototype blade with loading points bonded into the top and bottom surface. The blade was loaded through a loading head and whipple tree connected to an overhead jack in a way that simulated the combination of aerodynamic and centrifugal loads. Measurements of deflection were made using twelve dial gauges on the spoke plus blade assembly and strain readings made using two gauges fixed at either end of the flange which supported the leading edge of the blade on the fabricated steel spoke. The sides of the steel spoke containing the large cut-outs were coated

with brittle lacquer. The measured stresses and deflections were as anticipated and are shown in Ref A1.

A.1.4 Design specification

A.1.4.1 Dimensions and loadings

Number of blades - 10

Chord (c) 3.031 ft

Thickness (t) = $\frac{1.3c}{r-3.5}$ ft

Section - Clark Y

r (ft)	t (ft)	β (deg)	Aerodynamic axial force lb/ft	Aerodynamic circumferential force lb/ft
10.16125	0.5915	23.37	853.7	385.1
11.00	0.5253	21.90	925.7	382.6
12.00	0.4635	20.51	1012.0	381.5
13.00	0.4147	19.18	1115.5	381.2
14.00	0.3752	17.20	1265.7	376.9
15.00	0.3426	15.29	1436.4	364.6
16.00	0.3152	13.48	1607.6	347.8
16.50	0.3031	12.61	1693.1	337.7

β = inclination of fan blade to plane of rotation

The above loadings are maximum loadings at 2.2 atmospheres, 310 rev/min. Other extreme tunnel conditions considered in the design are:

1.0 atmospheres, 310 rev/min, aerodynamic loads 0.467 maximum

3.0 atmospheres, 263 rev/min, aerodynamic loads 0.848 maximum

A.1.5 Data summary (blades as made)

No. of fan blades	- 10
No. of prerotation vanes	- 21
No. of straightener vanes	- 9
Blade aerofoil section	- Clark Y series
Section thickness	- 20% (approx) at root; 10% at tip with linear variation
Chord length of blades	- 0.90 m
Nominal fan diameter	- 10.06 m
Nominal nacelle diameter at fan	- 6.19 m
Blade setting angle (chord to plane of rotation)	- 23.37° root; 12.61° tip

Nominal maximum rotational speed - 310 rev/min (clockwise when viewed from upstream)

Prerotation vane aerofoil section - NACA 6712

Straightener vane aerofoil section - RAF 30

REFERENCE

No.	Author	Title, etc
A.1		Tensile tests on a fan blade. Report for Department of Environment, National Engineering Laboratory. Report Z2/DOT/1/DMW January 1974

STN No	Radius in	Skin thickness	y_c	x_c	ΣAy^2 in^4	ΣAx^2 in^4	Ixy	Mass lb	EFF radius in	Rad from attach^t face	EI_{yy} lb in	GJ lb in
0	117 50	0 64	- 2.79	-16 54	383	6107	-406	16 25	119 7	9 7	612×10^6	947×10^6
1	121 95	0 59	- 2 73	- 16 44	318	5700	-318				509×10^6	870×10^6
1	121 95	0 545	- 2 72	- 16 41	295	5609	-289	33 23	126 92	16 92	472×10^6	822×10^6
2	132	0 545	- 2 43	- 16 55	217	5089	- 282				347×10^6	635×10^6
2	132	0 496	- 2 40	- 16 52	205	4899	-249	36 09	137 95	27 95	328×10^6	592×10^6
3	144	0 496	- 2 16	- 16 48	153	4341	-18[illegible]				245×10^6	458×10^6
3	144	0 45	- 2 17	- 16 48	141	4293	- 176	33 29	149 97	39 97	226×10^6	425×10^6
4	156	0 45	- 1 90	- 16 64	117	4186	- 165				187×10^6	335×10^6
4	156	0 405	- 1 80	- 16 61	107	3970	- 161	30 36	161 97	51 97	171×10^6	312×10^6
5	168	0 405	- 1 72	- 16 54	85	3764	- 149				136×10^6	248×10^6
5	168	0 357	- 1 72	- 16 50	76	3476	- 134	27 41	173 97	63 97	122×10^6	230×10^6
6	180	0 357	- 1 53	- 16 57	61	3378	- 103				98×10^6	201×10^6
6	180	0 310	- 1 56	- 16 55	56	3206	- 101	24 9	185 97	75 97	90×10^6	172×10^6
7	192	0 310	- 1 44	- 16 59	48	3038	- 94				77×10^6	142×10^6
7	192	0 265	- 1 43	- 16 55	45	2836	- 92	6 31	196 5	86 5	72×10^6	128×10^6
85"	195	0 265	- 1 40	- 16 57	43	2800	- 90				69×10^6	
85"	195	Balsa	- 1 40	- 15 6	82	7450	-					
8	198	Balsa	- 1 40	- 15 6	77	7312	-					

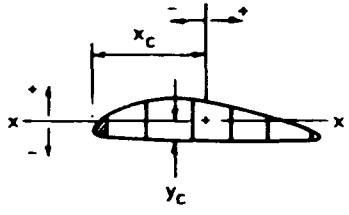

Shear centre calculated as 16.75in from LE for station No 1

Fig A1 5m fan blade section properties

Appendix

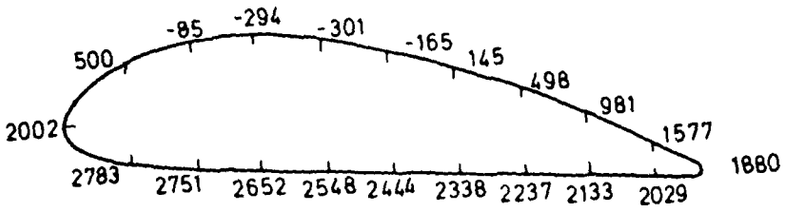

a) 2.2 atmos 310 rpm

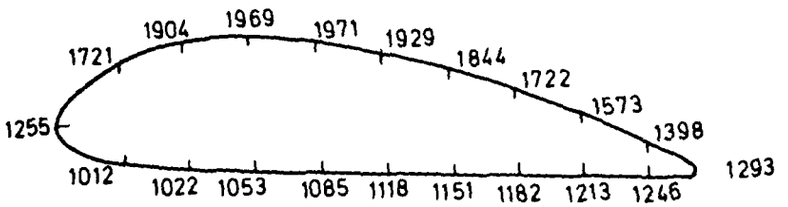

b) 1.0 atmos 310 rpm

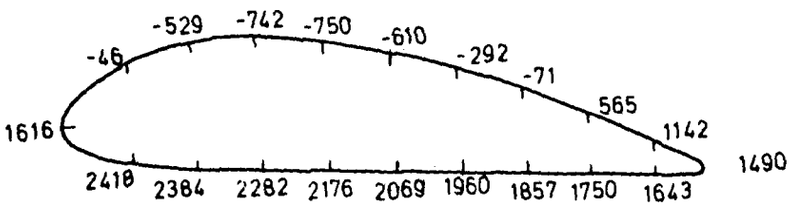

c) 3 atmos 263 rpm

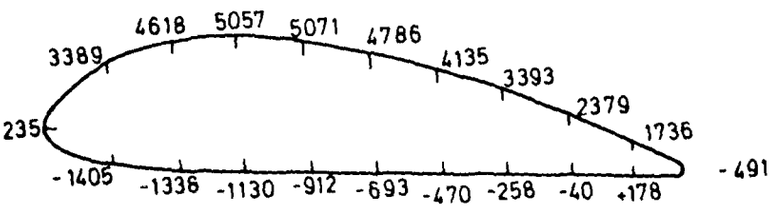

d) No air load 310 rpm (off design case)

Fig A2 Stresses in skin at station 0 (junction with flange)

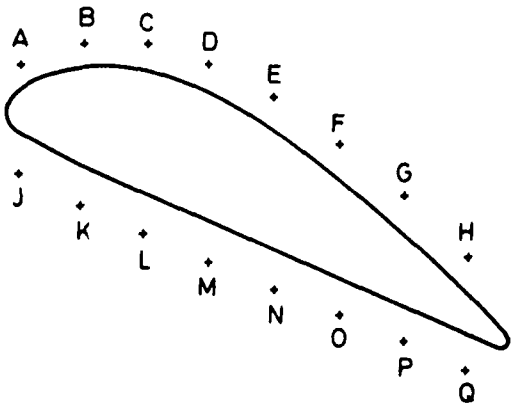

Bolt Ref	2.2 atmos 310 rpm	1 atmos 310 rpm	3 atmos 263 rpm	Off design no air BM 310 rpm
A	7343	7758	5173	◆ 8014
B	6292	8479	3932	◆ 9826
C	5770	8838	3313	◆ 10999
D	5549	8990	3052	◆ 11110
E	5538	8997	3041	◆ 11127
F	5741	8858	3280	◆ 10778
G	6107	8606	3954	◆ 9794
H	6677	8214	4388	◆ 9160
J	9482	8290	7700	◆ 4324
K	9497	8279	7719	◆ 4297
L	9392	8351	7595	◆ 4477
M	9279	8428	7462	◆ 4672
N	9167	8506	7329	◆ 4866
O	9066	8575	7210	◆ 5310
P	8943	6660	7064	◆ 5253

(Bolts iso metric grade 10 9
Proof load = 77 823 lb
Torqued load = 52 000 lb
Max bolt load (design condition) = 9 500 lb
∴ FOS = 5.5 on torqued load
8 1 on proof load)

Fig A3 Loads on attachment bolts (lb)

Station No	Radius (in)	CF (lb)	Resultant of air loads 2.2 atmos	BM due to air load
0	117.5	5331	Non eff^{ve}	372693
1	121.95	11385	776.3	337084
2	132	13624	1039.9	260269
3	144	13594	1131.9	179888
4	156	13379	1249.1	112523
5	168	13005	1393.7	59417
6	180	12514	1555.5	22140
7	192	3585	840.7	2545
8	198			
	Total	86417	7987	

Blade inclined so that
CF bending moment =
0.684 air bending moment
at each station

Fig A4 Aerodynamic and centrifugal loads on blade at 310 rev/min (case 1, 2.2 atmos)

043

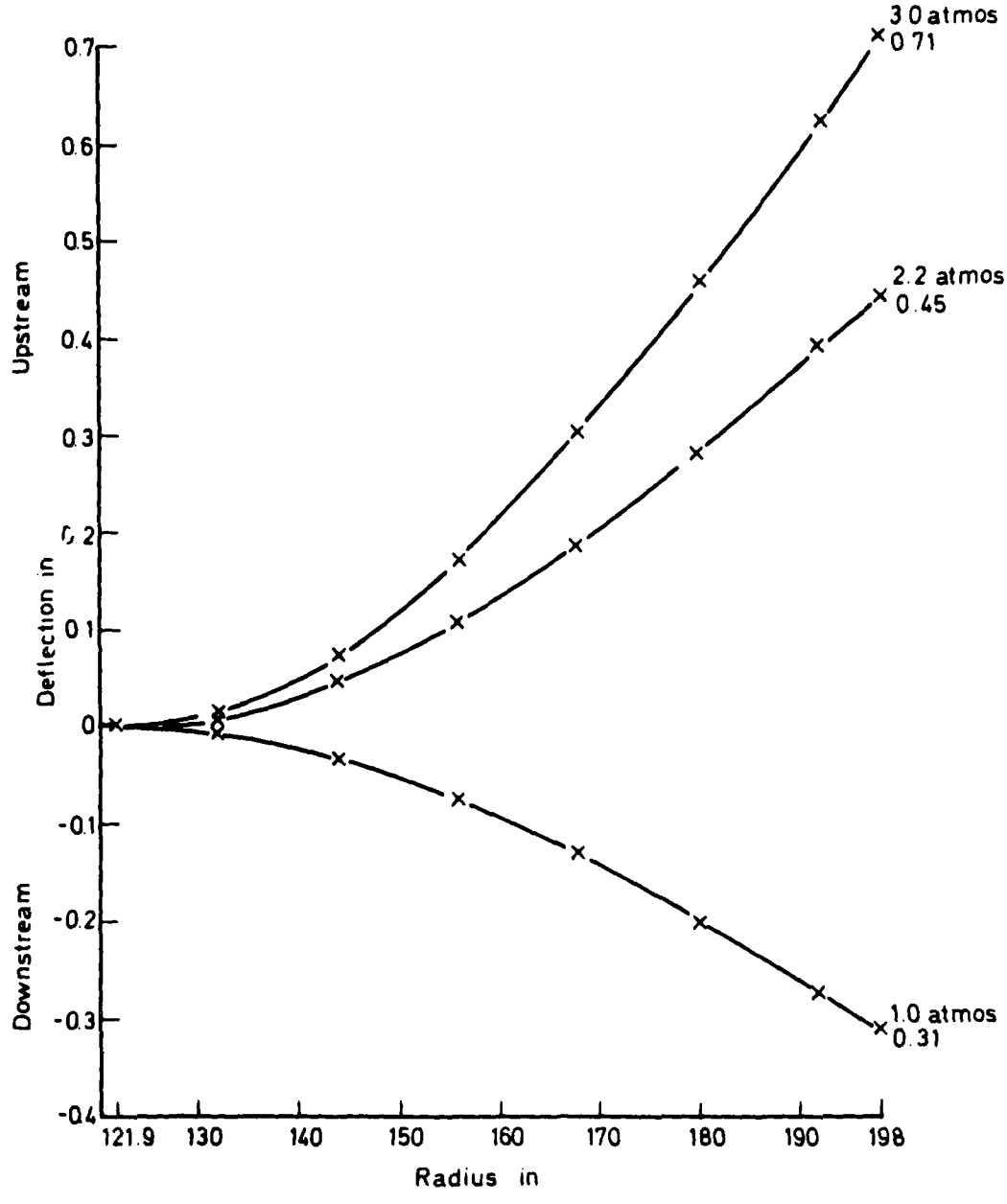

Fig A5 Estimated deflection of blade (normal to local chord)

Station	Radius from ℄	Design	2.2 atmos Deflection°	310 rpm Angle	1.0 atmos Deflection°	310 rpm Angle	3 atmos Deflection°	263 rpm Angle
1	121.9	30.37	0	30.37	0	30.37	0	30.37
2	132	21.90	+0.02	21.92	-0.01	21.89	0	21.90
3	144	20.51	+0.03	20.54	-0.01	20.50	+0.01	20.52
4	156	19.18	+0.05	19.23	-0.02	19.16	+0.02	19.20
5	168	17.20	+0.08	17.28	-0.01	17.19	+0.03	17.23
6	180	15.29	+0.10	15.39	0	15.29	+0.04	15.33
7	192	13.48	+0.12	13.60	0	13.48	+0.05	13.53
8	198	12.61	+0.13	12.74	0	12.61	+0.06	12.67

Fig A6 Estimated angles of blade, with twist due to centrifugal forces and air loads

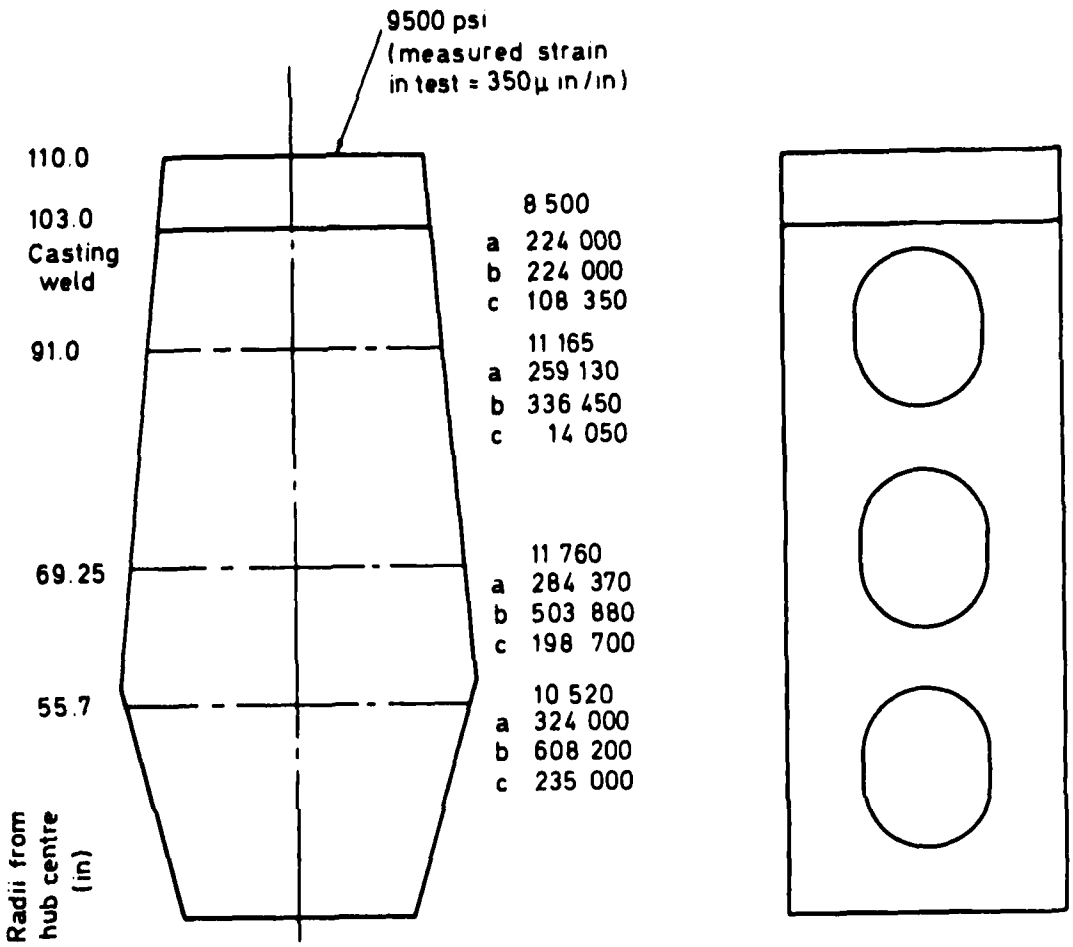

Stress for worst corner lb/sq in

Loading a CF due to mass outside section (lb)

b Resultant of axial air BM & CF BM lb in

c Circumferential air BM & CF BM lb in

Stressess stated are those on worst corner, 310 rpm, 2.2 atmos

Fig A7 Estimated loads and stresses on spoke

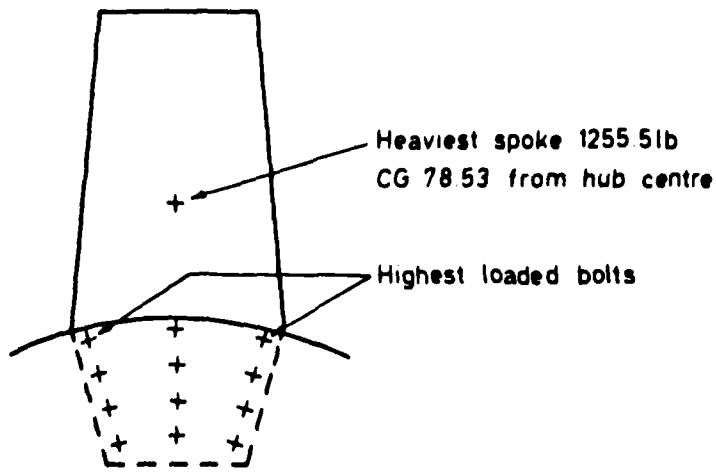

CF 310 rpm
Spoke = 159 810 lb in
Blade fairings, bolts etc = 132 220
CF force / bolt = 12168
Resultant BM (air load and CF bending) 889120
B M force / bolt 2861
Shear coupling break point set at 72 500 kgm = 524 175 ft lb
ie each spoke absorbs 52 420 ft lb
Assuming whole torque absorbed by inertia of spokes
resulting shear on highest loaded bolt = 714 lb
Resultant shear load, highest loaded bolt = 15 050 lb
Shear stress = 4.26 tons / sq in
Bearing stress = 7.5 tons / sq in
(bolts are torque tightened as friction grip bolts to BS 3294)

043

Fig A8 Loads and stresses in spoke attachment bolts

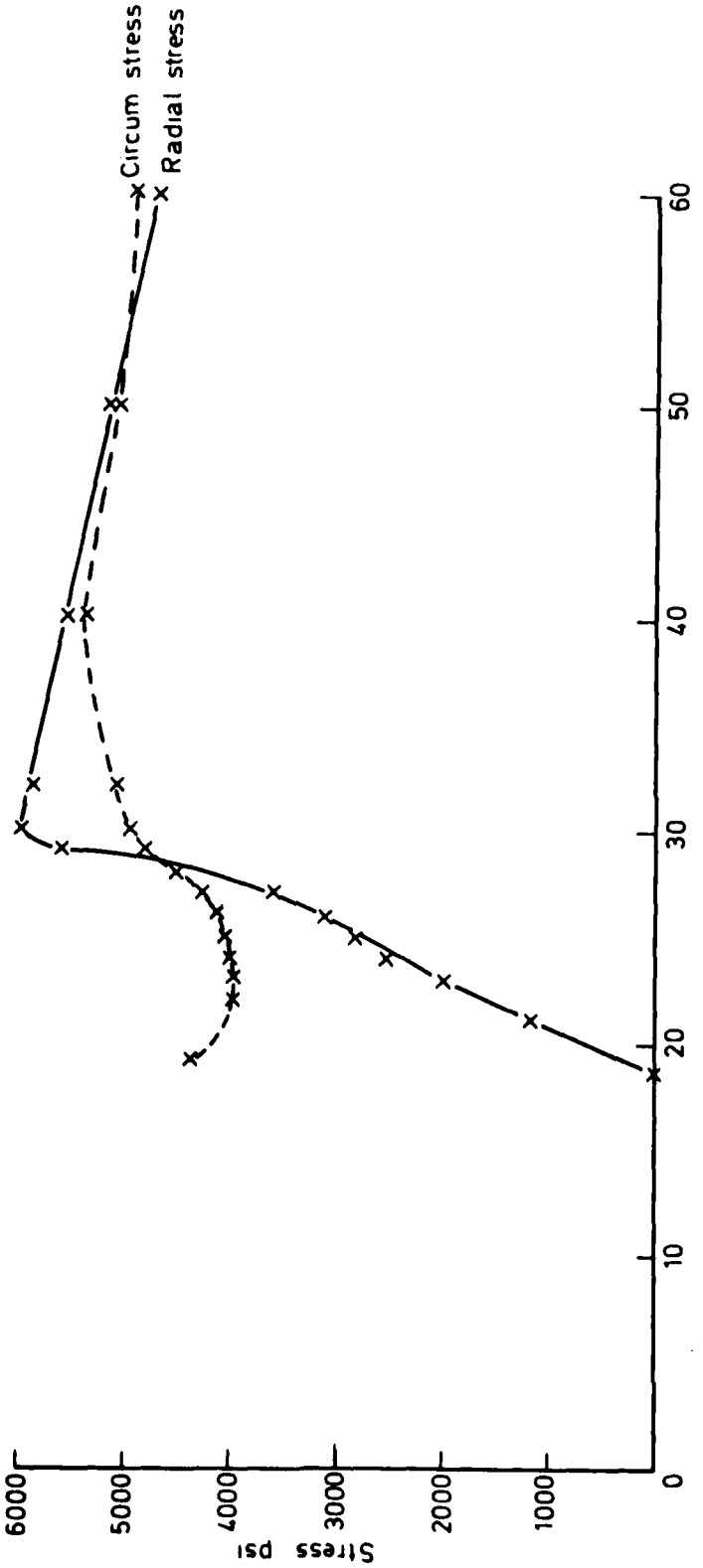

Fig A9 Stresses in hub disc

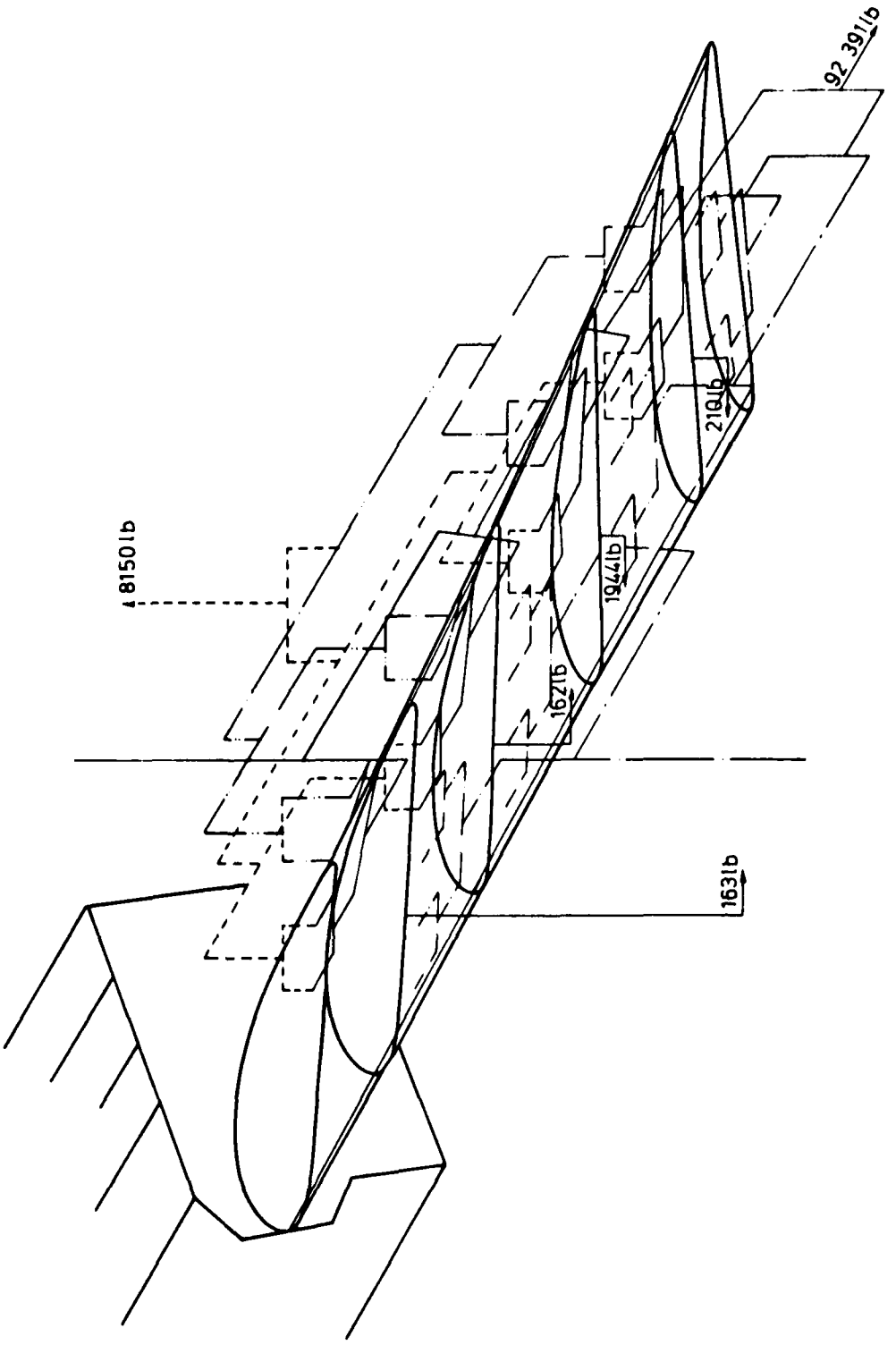

Fig A10 Fan blade test

REFERENCES

No.	Author	Title, etc
1	A. Spence D.S. Woodward M.T. Caiger A.J. Sadler R.W. Jeffery	The 5m pressurised low speed wind tunnel. ICAS Conference, Lisbon, Paper B3-05 (1978)
2	W.A. Mair	The design of fans and guide vanes for high speed wind tunnels. Br ARC R&M 2435 (1944)
3	A.J. Sadler	Model tests of the fan for the 5m tunnel. RAE unpublished
4	S.T. Parkinson	Resonance tests on a fan blade for the RAE 5m wind tunnel. RAE unpublished
5	G.A. Taylor D.R. Gaukroger C.W. Skingle	MAMA - a semi-automatic technique for exciting the principle modes of vibration of complex structures. RAE Technical Report 67211 (1967)
6	J.A. Copley	RAE Structures Department. Private communication
7	C.W. Skingle K.H. Heron D.R. Gaukroger	Numerical analysis of vector response loci. RAE Technical Report 73001 (1973)
8	R.A. Robinson J.C. Childers D.I. Yando	Analysis of the rotor blade vibratory stresses of the propulsion wind tunnel compressors. Naval Research Laboratory, Shock and Vibration Bulletin No. 35 January 1966
9	C.J.W. Hassal	Development and initial application of a technique to measure vibration mode shapes of a rotating blade. RAE Technical Report 77064 (1977)

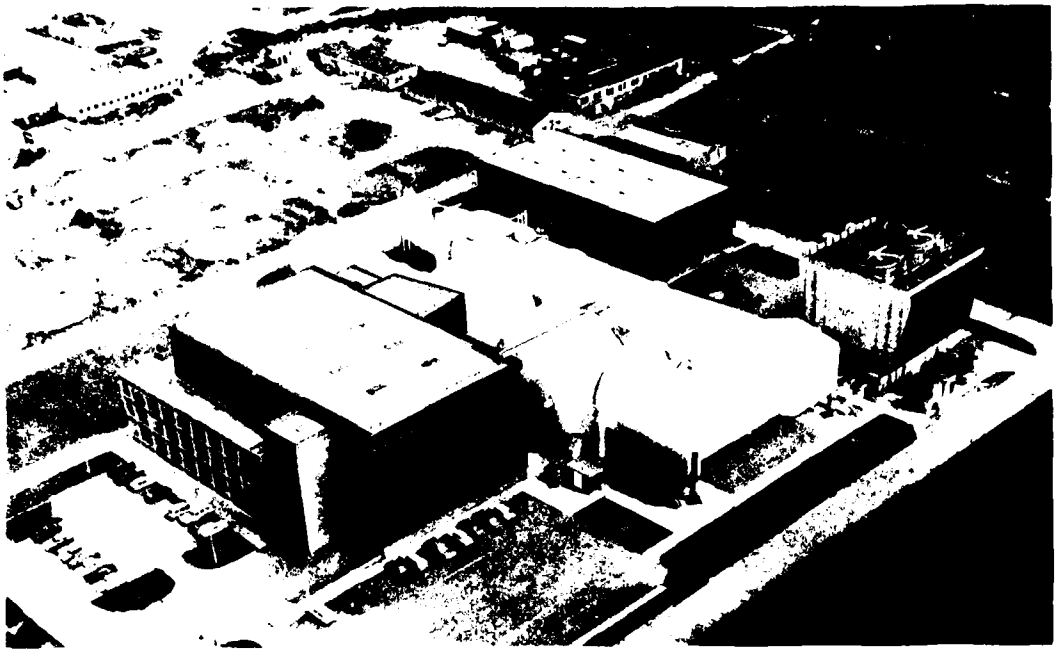

Fig 1 Aerial view of 5 metre tunnel

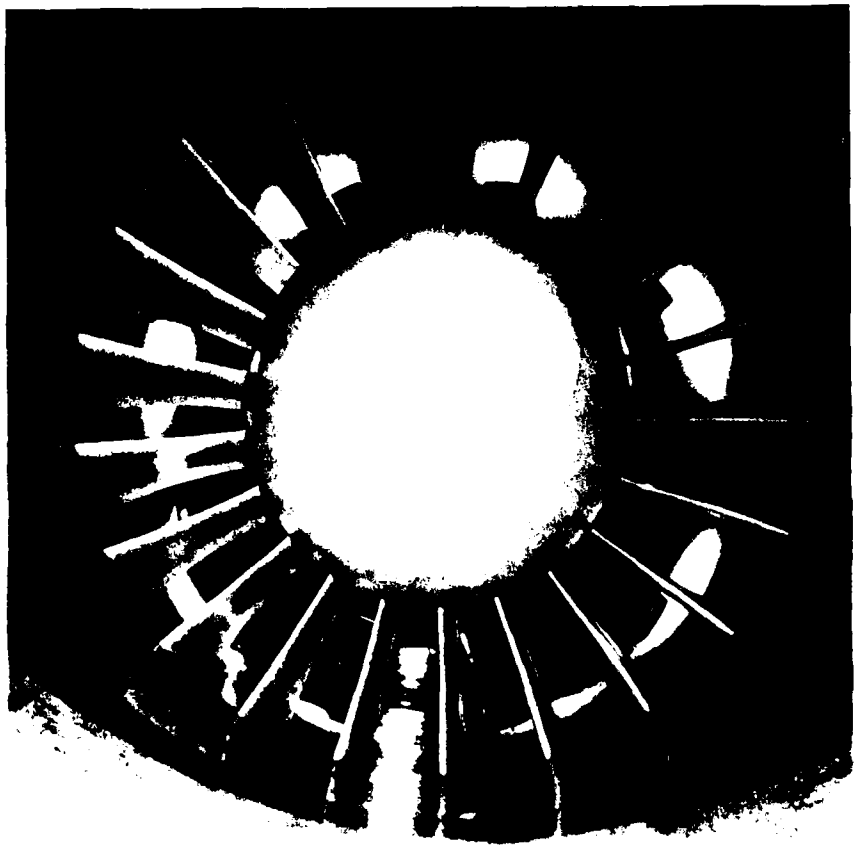

Fig 2 General view of fan and nacelle assembly

TR 80043 C16181

Blade number

Mode number	1	2	3	4	5	6	7	8	9	10	11	12	13	14	15
1	23.6 0.6	23.5 0.6	23.5 0.6	23.5 0.7	23.8 0.6	23.6 0.5	23.5 0.6	23.3 0.64	23.7 0.76	23.6 0.56	23.1 0.65	23.4 0.42	23.7 0.63	23.5 0.64	23.4 0.64
2	73.5 1.6	76.5 1.6	77.7 1.6	77.2 1.9	76.5 1.5	75.2 1.7	72.? 1.1	75.4 1.29	76.3 1.37	72.9 1.85	75.8 1.72	76.8 1.56	76.0 2.1	76.6 1.52	76.9 1.63
3	101.5 1.4	103.0 1.6	103.4 1.6	99.6 1.7	99.4 1.7	99.3	99.8 1.9	101.4 2.74	103.7 1.56	102.0 1.48	101.6	102.6	103.7	100.7	91.7
4	163.5 0.9	160.6 0.8	160.5 0.7	158.2 0.9	157.0	155.7	156.6 0.8	155.7 0.79	157.3 0.81	158.4 0.79	156.8	157.5	158.4	157.4	157.9
5	217.2 0.7	205.4	205.3	204.1	202.3	200.1	203.1 0.8	207.4	210.3	204.1 0.85	203.3	218.8	211.6	210.1	200.6
6	252.3 0.8	248.0	249.0	244.6	243.1	241.7	242.4 0.8	241.0	245.1	243.5 0.85	242.2	246.5	248.3	245.6	243.5
7	288.9 0.8	280.8	283.5	271.7	286.0	267.7	267.9	268.3	270.6	269.2 0.66	268.9	270.9	271.7	266.7	273.6
8	302.1 1.4	299.0	294.2	298.5	294.9	288.1	282.0	295.0	291.1	284.8 0.88	302.1	293.7	294.1	300.7	281.1
9	333.1 1.3	333.3	351.1	333.1	333.3	329.7	331.0	333.6	339.8	331.9 0.85	341.4	339.8	340.4	333.5	340.2

The upper figure in each mode per blade is mode natural frequency (Hertz), the lower figure is percent critical damping

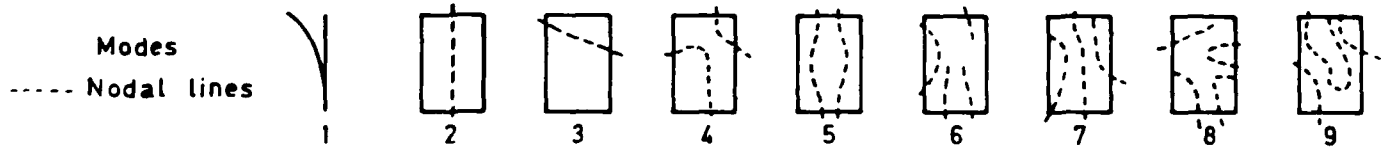

Fig 3 Frequency, damping and mode shape for all blades

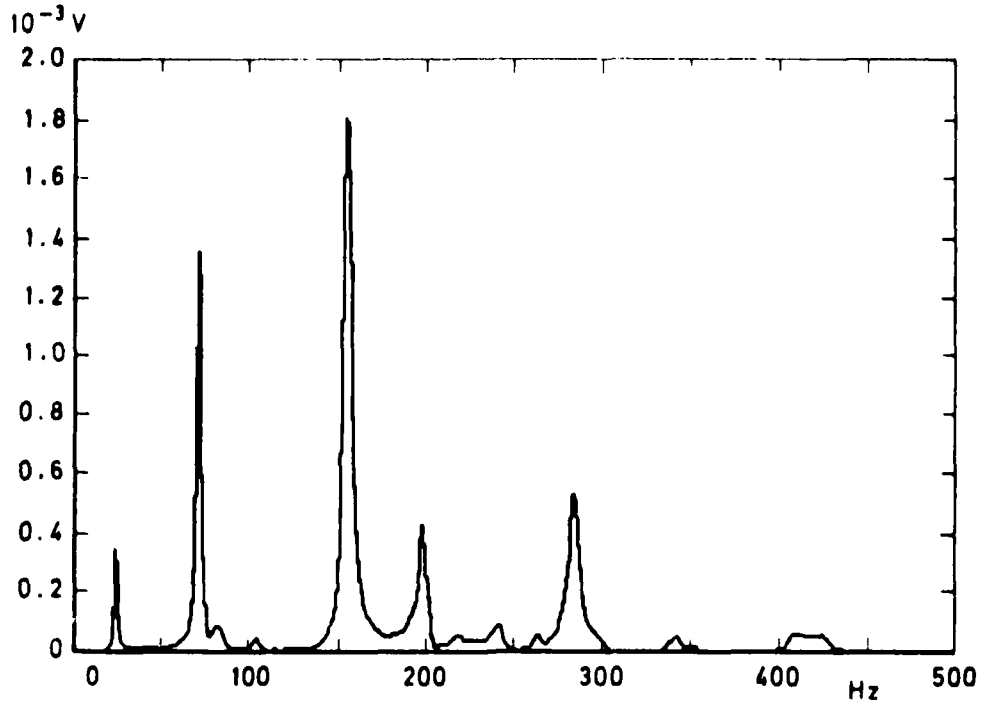

a) Leading edge transducer

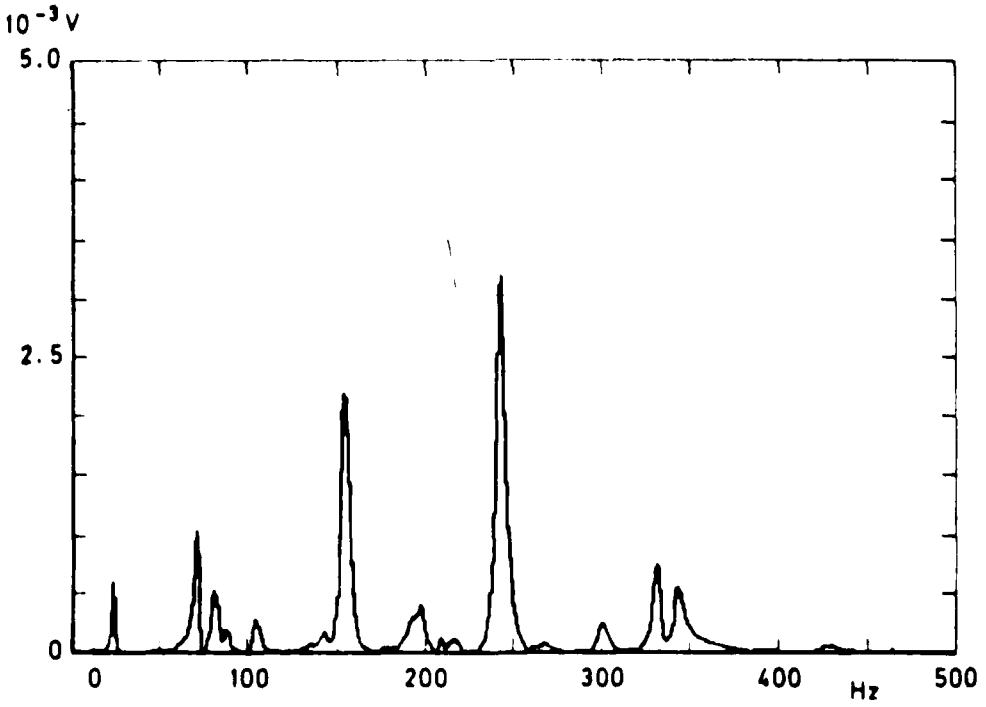

b) Trailing edge transducer

TR 80043

Fig 4a&b Response of blade to trailing edge hit

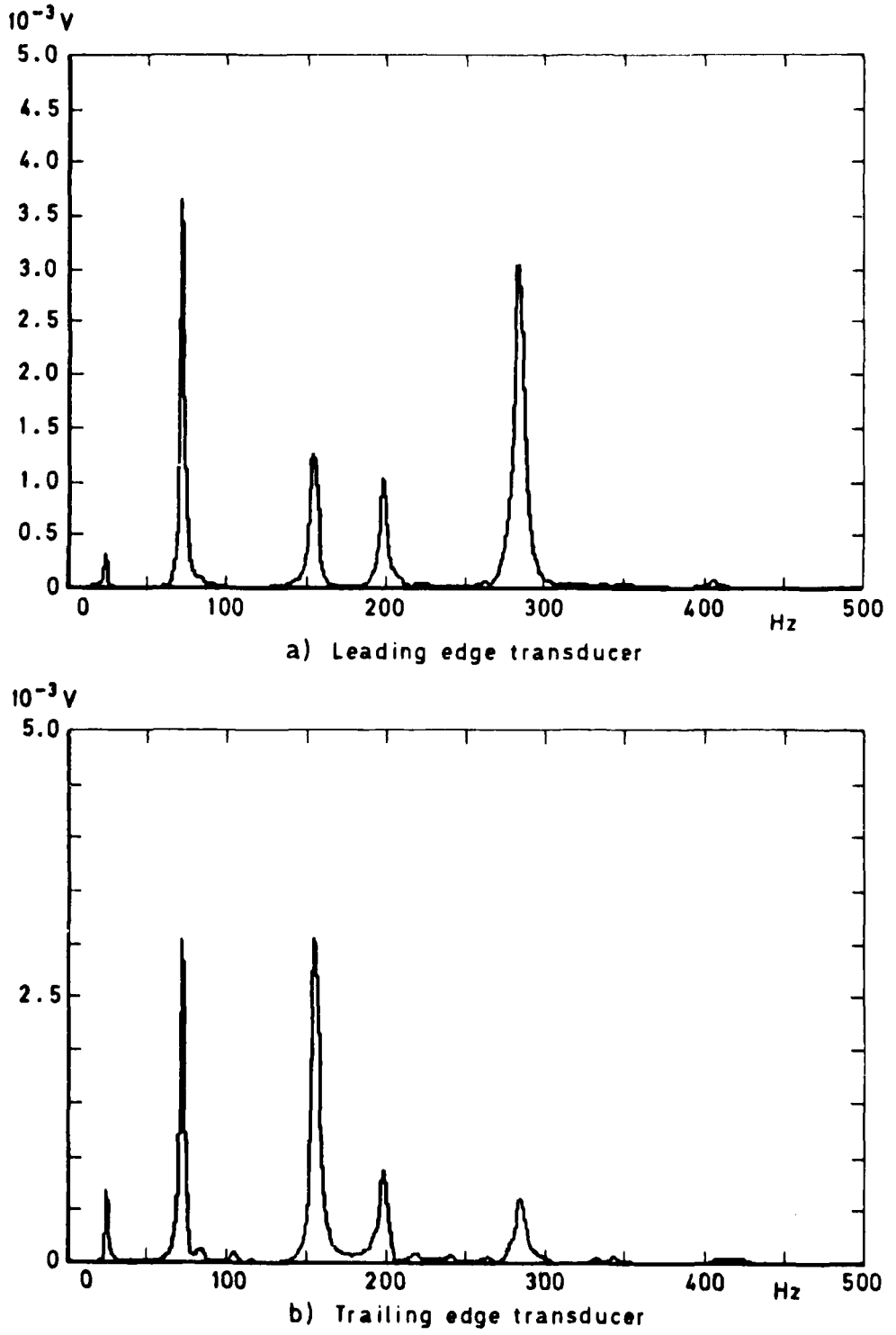

Fig 5a&b Response of blade to leading edge hit

TR 80043

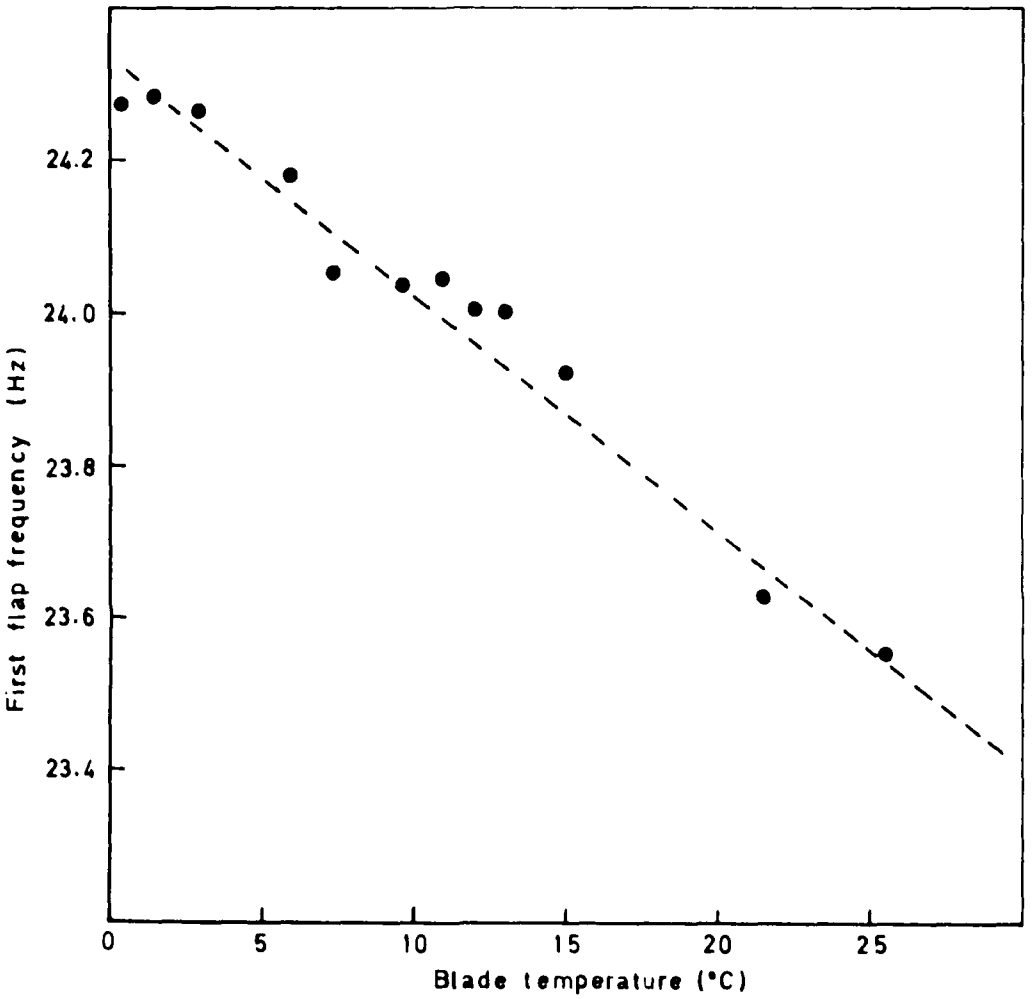

Fig 6 Variation of first flap frequency with blade temperature (Blade 8)

Fig 7

Date	Hours run	Average frequency over 10 blades (Hz)	Blade temperature (°C)	$R_x = f_x / 0.1 \sum_{z=1}^{10} f_z$ for each blade										
				8	14	10	3	'	5	11	6	12	4	9
29.11.77	Datum	24.247		1.004	1.001		0.997	1.000	1.002	0.998	1.001	1.000	0.996	1.001
2.12.77	1.3	24.063		1.004	1.001		0.997	0.999	1.001	0.998	1.001	1.000	0.998	1.001
6.12.77	4.5	24.045		1.003	1.002		0.998	1.000	1.002	0.997	1.001	1.000	0.997	1.001
13.12.77	10.0	23.628		1.003	1.002		0.999	0.999	1.001	0.997	1.001	0.999	0.997	1.000
11. 1.78	21.0	24.053		1.002	1.001		0.996	1.003	1.003	0.998	1.002	1.000	0.996	1.000
10. 2.78	41.9	24.214	0.4	1.002	1.000		0.997	0.999	1.002	0.997	1.003	1.000	0.998	1.001
15. 2.78	48.4	24.131	3.0	1.005	1.003		0.999	1.000	1.001	0.995	1.000	0.998	0.997	1.002
17. 2.78	52.7	23.998	7.4	1.003	1.000		0.997	0.998	1.002	0.998	1.003	1.000	0.998	1.001
22. 2.78	52.7	23.995	9.6	1.003		1.004	0.998	1.000	1.002	0.997	1.001	0.998	0.996	1.000
8. 3.78	64.0	23.579	25.5	1.002	1.001		0.997	0.999	1.003	1.000	1.004	0.999	0.997	0.999
20. 3.78	87.4	23.909	21.5	1.005	1.003		0.998	0.998	1.001	0.997	1.001	0.998	0.997	1.002
1. 4.78	106.8	23.990	11.0	1.005	1.001		0.997	0.997	1.003	0.998	1.001	0.999	0.998	1.002
9. 5.78	171.6	23.784	15.0	1.006	1.001		0.996	0.998	1.002	0.996	1.003	0.999	0.997	1.003
4. 7.78	244.5	23.893	13.0	1.004	1.001		0.997	0.998	1.002	0.996	1.003	1.000	0.997	1.003
27.11.78	347.3	24.226	1.5	1.003	1.001		0.997	0.997	1.003	0.998	1.000	1.000	0.998	1.002
8. 3.79	245.8	24.041	6.0	1.005	1.001		0.997	0.997	1.002	0.996	1.001	0.999	0.998	1.002
12. 5.79	563.9	23.917	12.0	1.004	1.001		0.998	0.998	1.001	0.996	1.001	0.998	0.997	1.002

				Percentage critical damping for each blade										
8. 3.78		23.579 LE	25.5	0.492	0.471		0.577	0.579	0.468	0.617	0.488	0.577	0.588	0.538
		TE		0.506	0.495		0.560	0.593	0.500	0.650	0.506	0.595	0.569	0.537
4. 7.78		23.893 LE	13.0	0.657	0.599		0.632	0.694	0.620	0.707	0.605	0.748	0.693	0.744
		TE		0.667	0.606		0.594	0.658	0.557	0.661	0.628	0.730	0.703	0.733

Fig 7 Variation of frequency and damping through maintenance checks to date (first flap mode)

Mode	Average frequency over the 10 blades	$R_x = f_x / 0.1 \sum_{z=1}^{10} f_z$ for each blade									
		8	14	3	7	5	11	6	12	4	9
FIRST FLAP MODE	23.951	1.004	1.001	0.997	0.999	1.002	0.997	1.002	0.999	0.997	1.001
	0.229	0.001	0.001	0.001	0.002	0.001	0.001	0.001	0.001	0.001	0.001
FIRST TORSION MODE	71.655	0.999	1.001	1.008	0.997	1.001	0.991	0.997	0.997	1.005	1.003
	1.067	0.003	0.003	0.004	0.004	0.005	0.007	0.004	0.002	0.003	0.002
SECOND TORSION MODE	158.08	0.981	0.998	1.020	1.002	0.997	0.995	0.998	0.996	1.006	1.008
	2.119	0.002	0.002	0.001	0.001	0.001	0.002	0.001	0.002	0.001	0.001

Fig 8 Summarised results of checks to date, for chosen modes

Fig 9

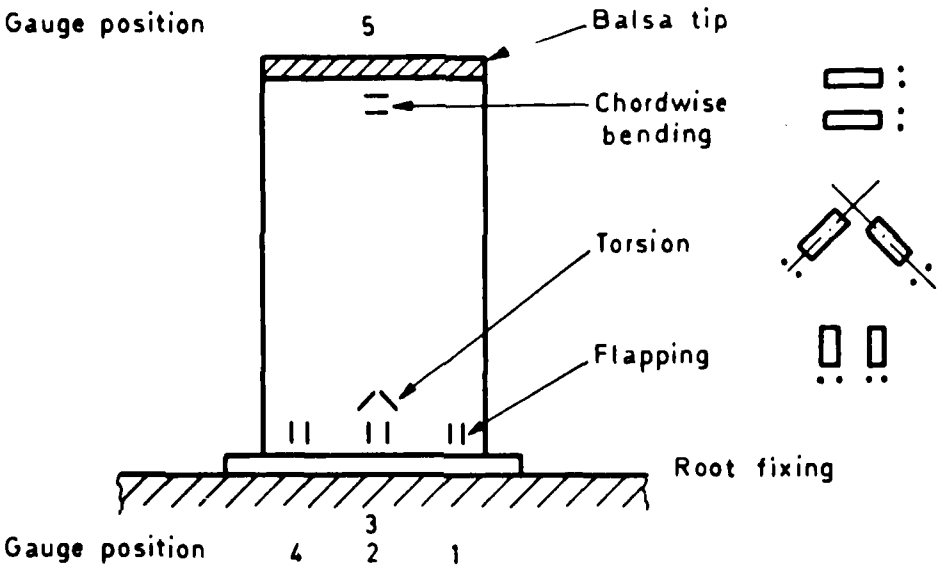

Gauge response to basic mode excitations

Excitation		Measured output (Volts)				
Mode	Frequency (Hz)	Gauge position				
		1	2	3	4	5
1	23.7	1.35 1.00	.15 .18	6.7 1.00	7.2 1.00	.32 .36
2	76.0	.60 0.44	.84 1.00	.17 .03	.66 .09	.90 1.00
3	101.3	.14 0.10	.07 .08	.34 .05	.38 .05	.20 .22
4	159.5	.36 0.27	.57 .68	.26 .04	1.00 .14	.84 .93
5	206.6	.36 0.27	.25 .30	.15 .02	.19 .03	.33 .37
6	245.3	.12 .09	.04 .05	.22 .03	.43 .06	.62 .69
7	284.7	.10 .07	.10 .12	.10 .01	.30 .04	.44 .49
8	303.1	.25 .19	.11 .13	.06 .01	.15 .02	.24 .27
9	343.4	.14 .10	.04 .05	.06 .01	.10 .01	.60 .67

Fig 9 Results of test to optimise gauge positions

TR 80043

Fig 10 Instrumented fan blade

Fig 11a&b

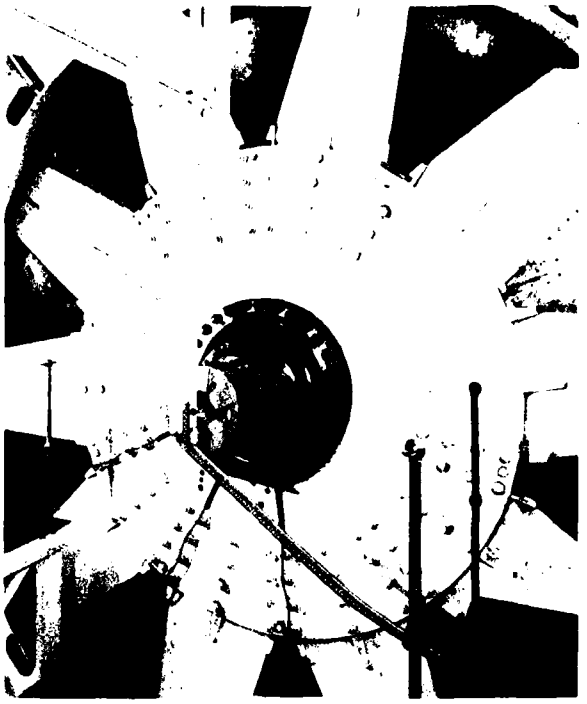

a

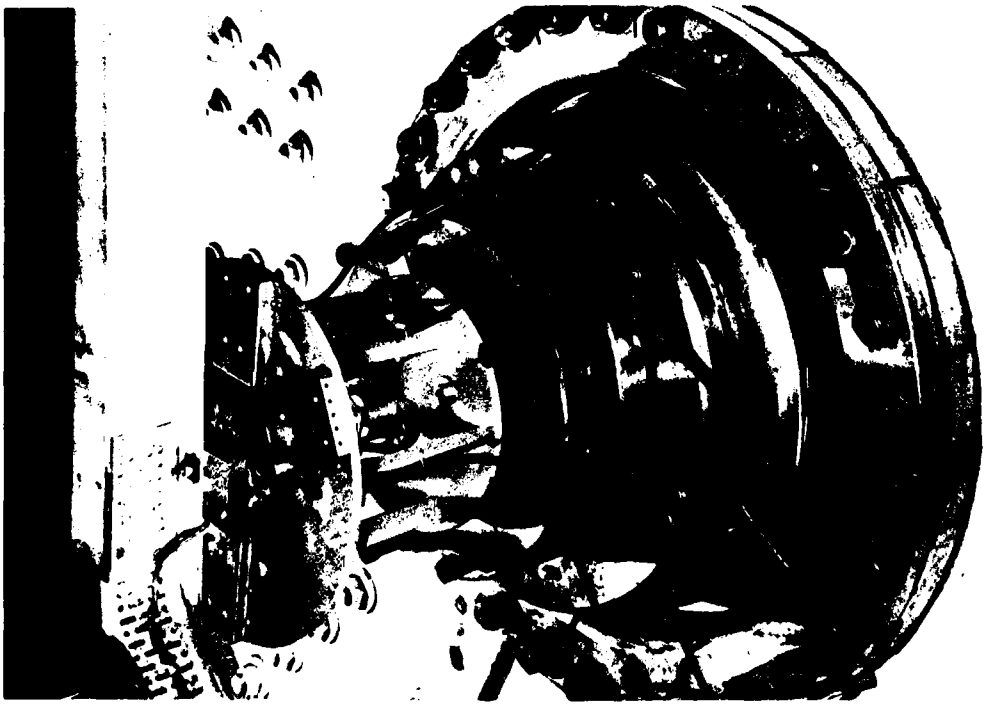

b

TR 80043

Fig 11a&b Hub, spoke and slip ring assembly

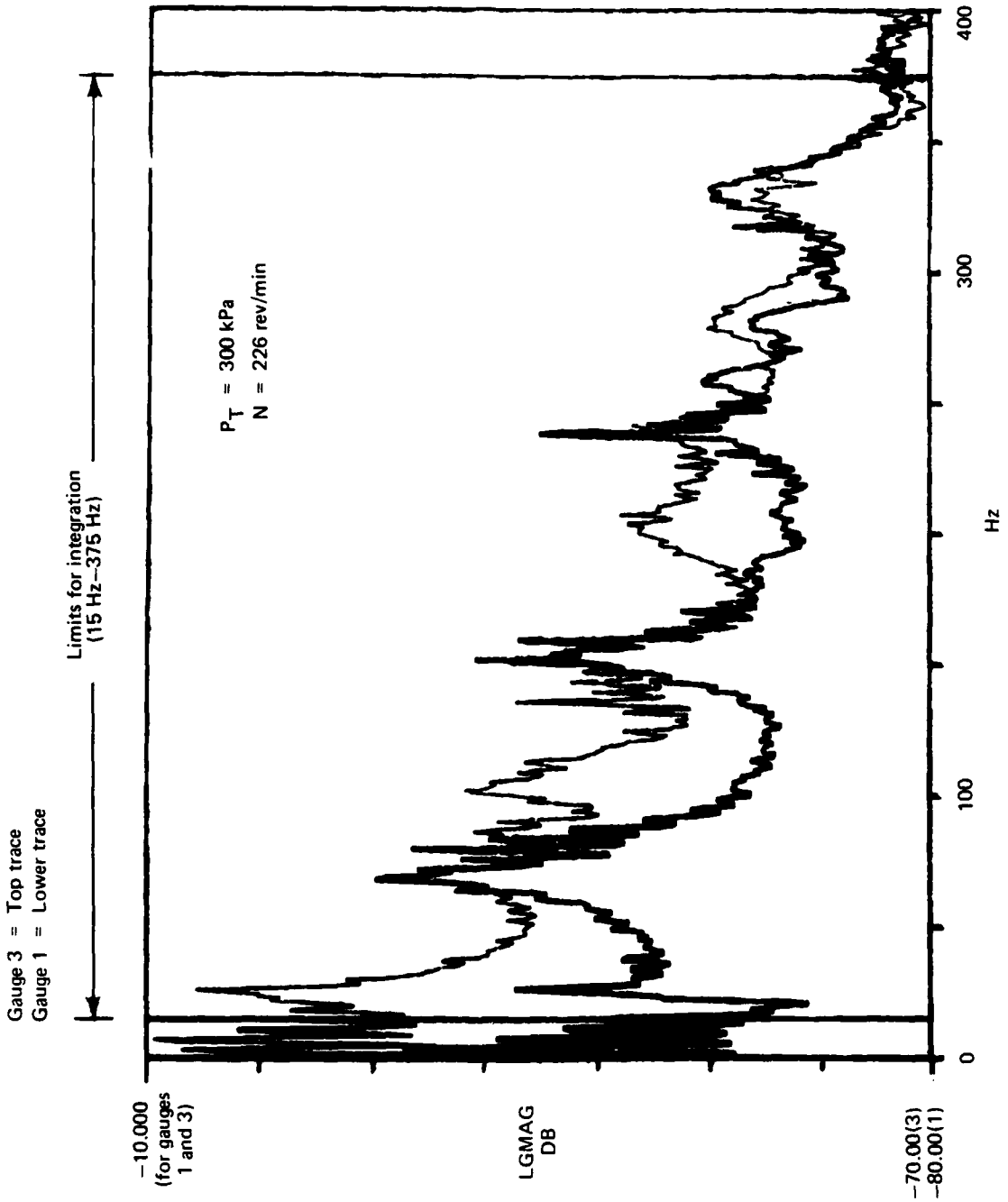

Fig 12 Spectra for both gauge positions

Fig 13

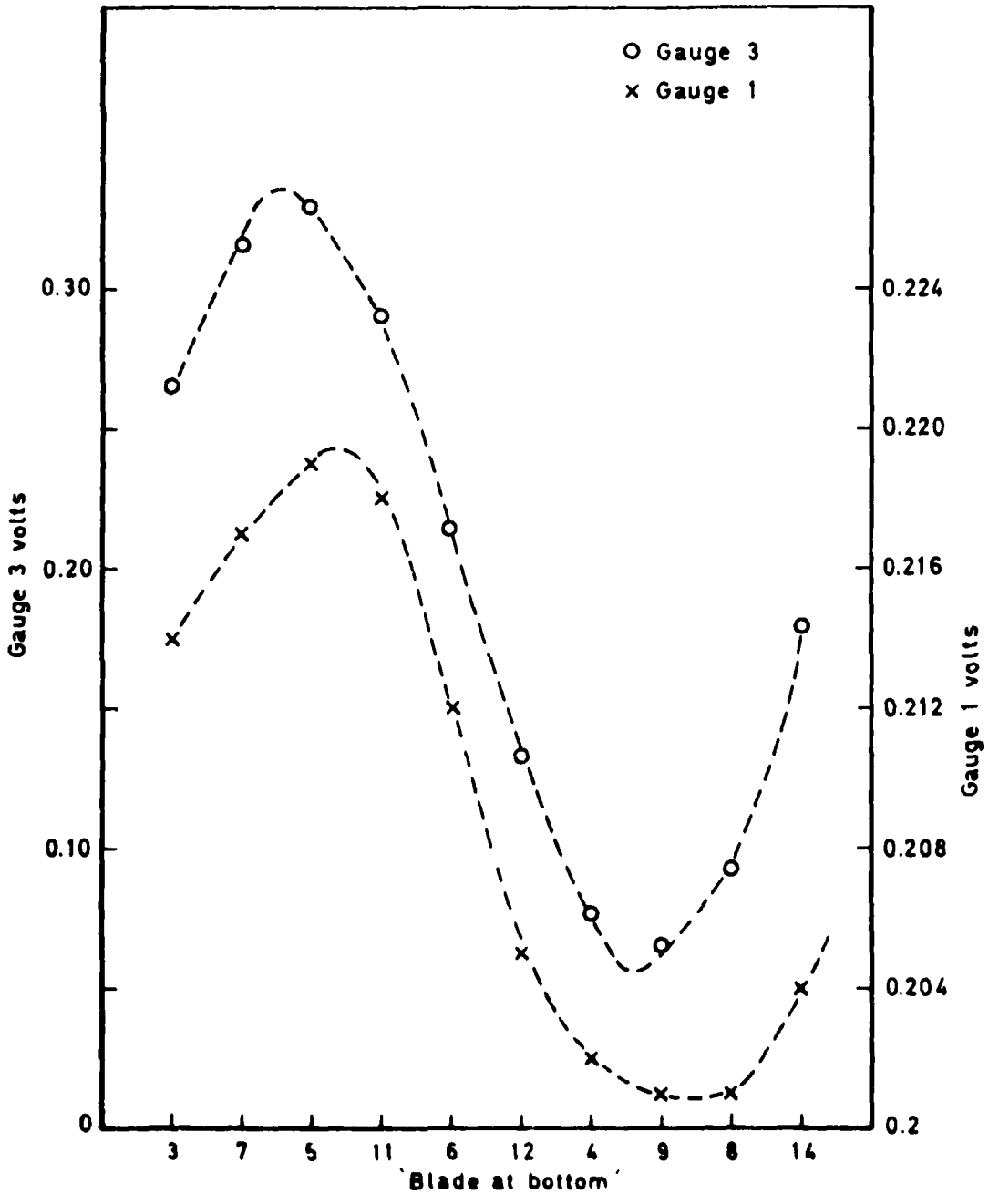

Fig 13 Strain gauge output for single revolution (Blade 11)

TR 80043

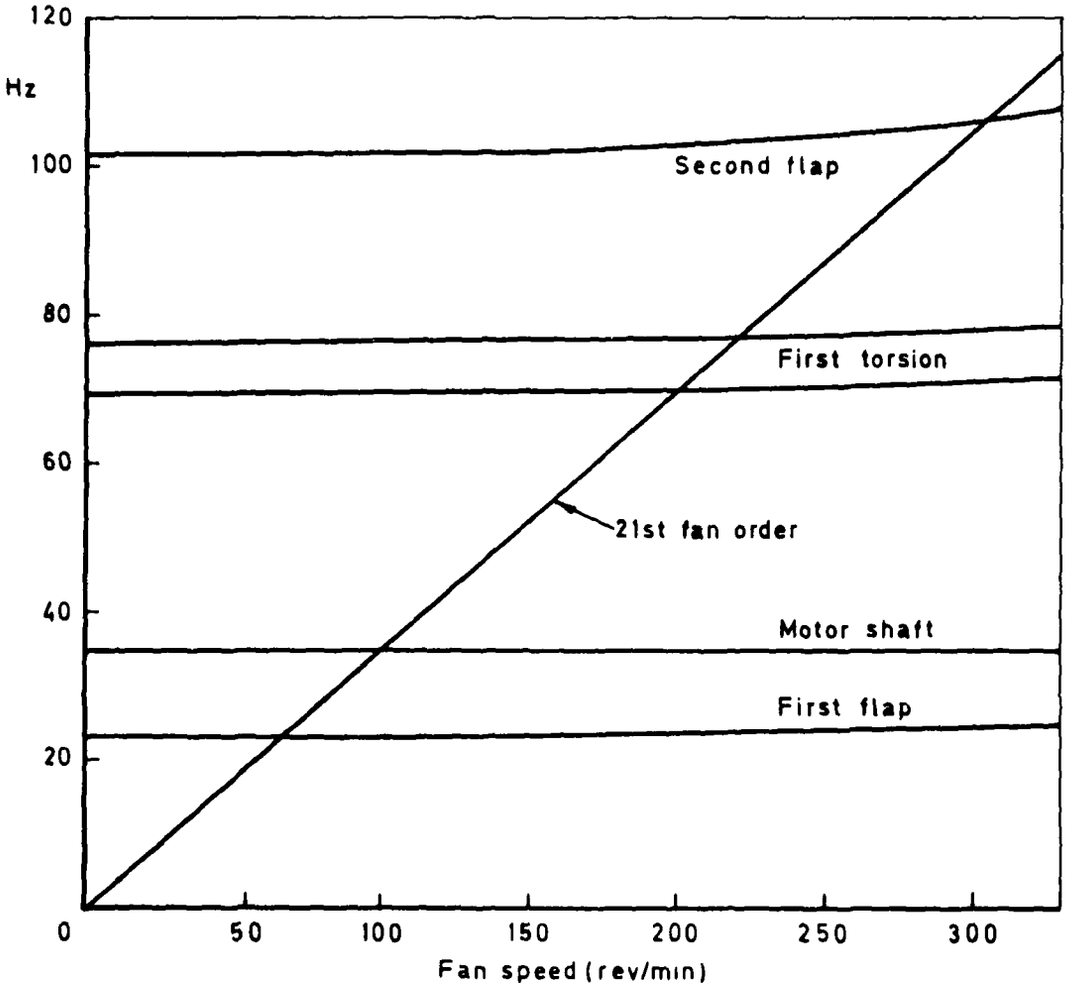

1A 80043

Fig 14 Interference diagram

Fig 15

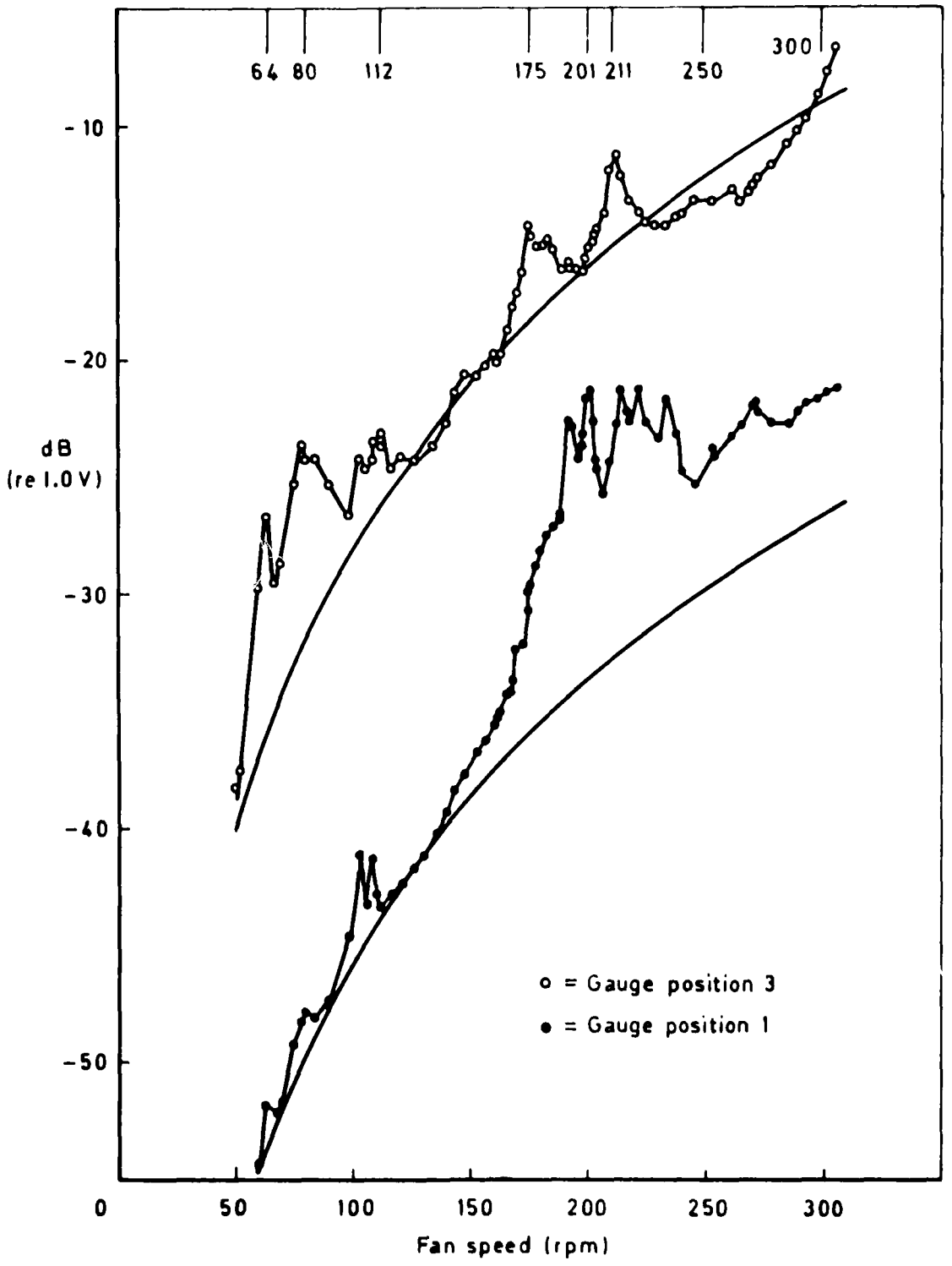

TR 80043

Fig 15 Fan blade response (atmospheric pressure)

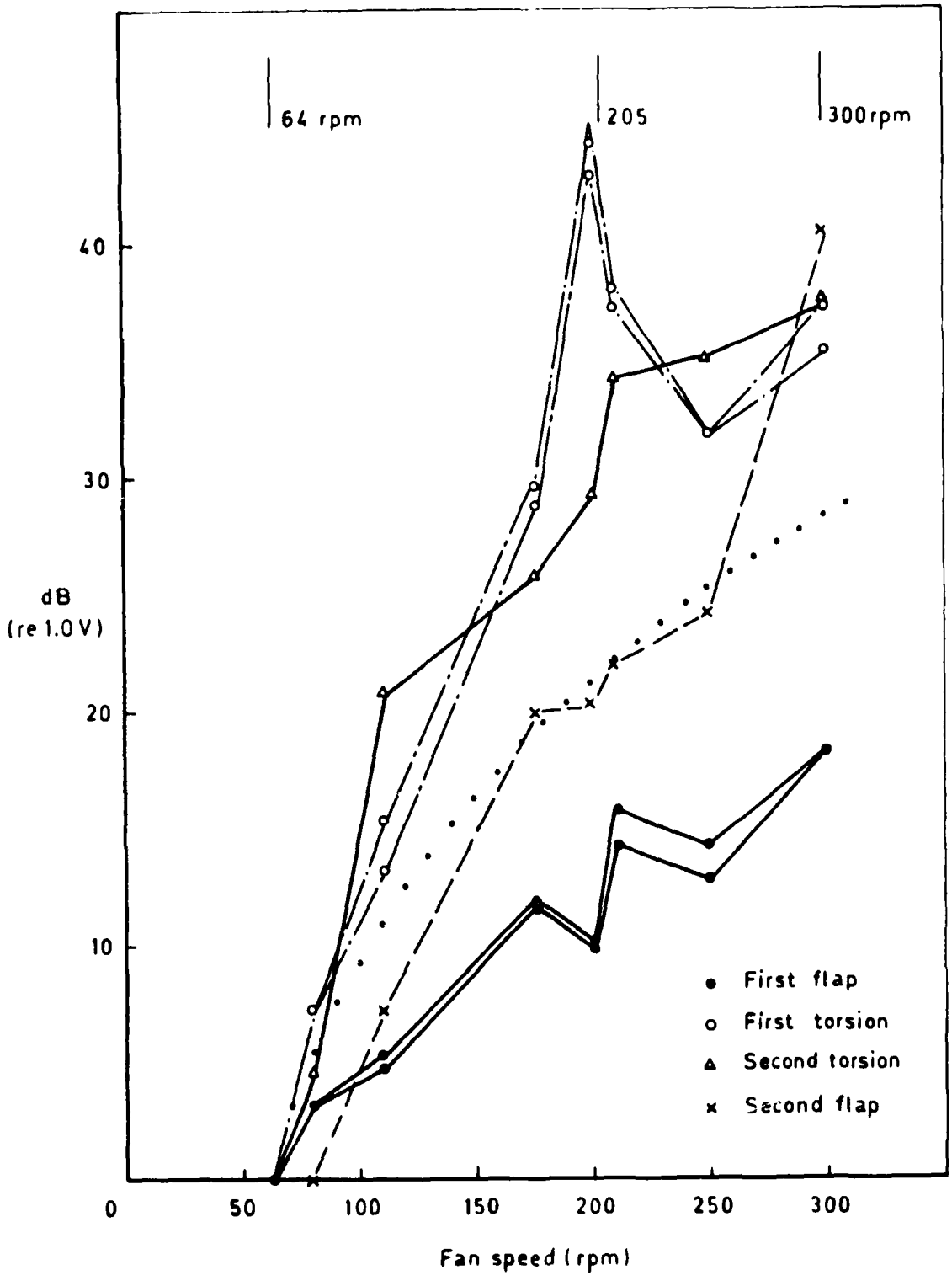

TR 80043

Fig 16 Fan blade resonance (atmospheric pressure)

Fig 17a

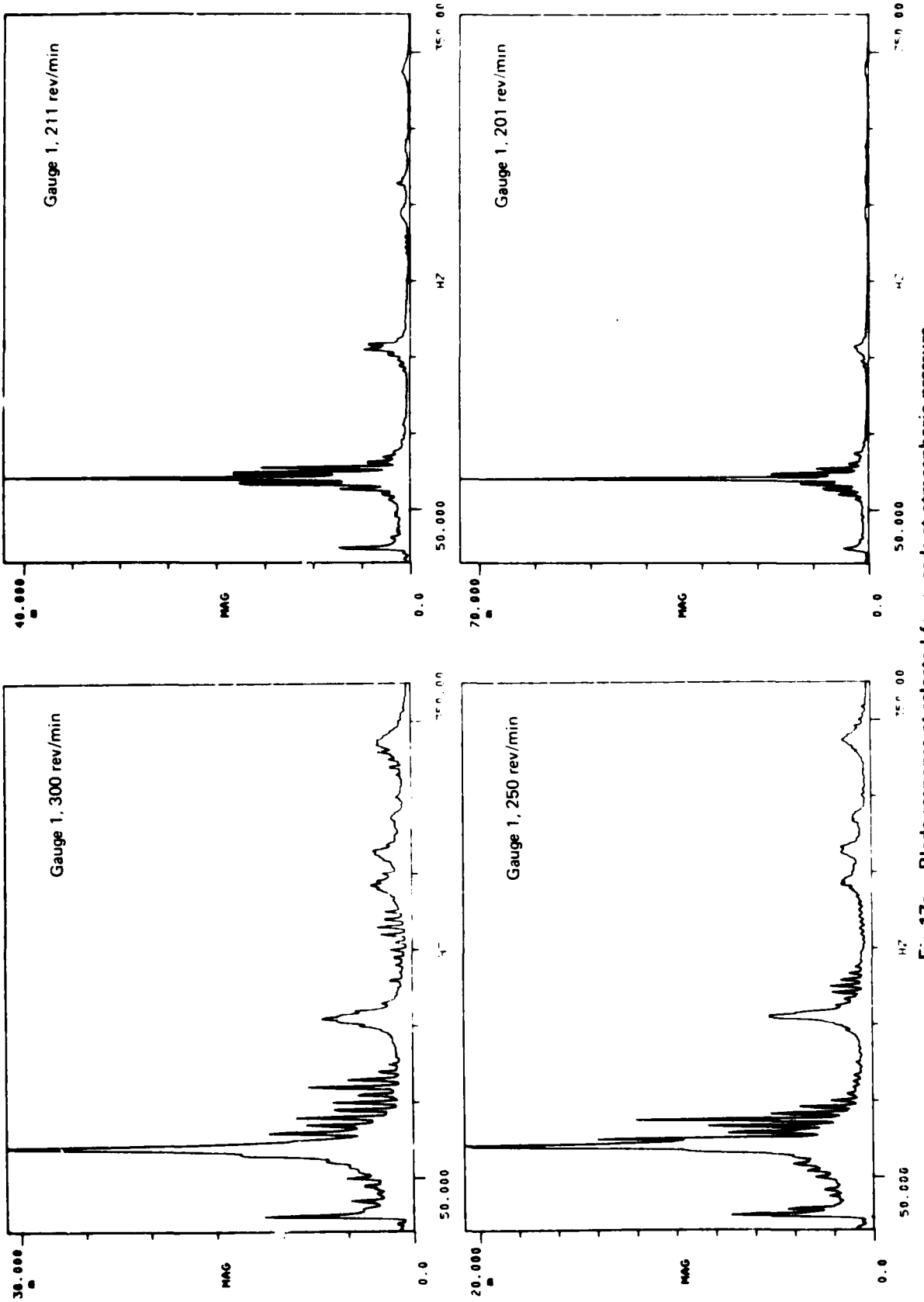

Fig 17a Blade response at selected fan speeds at atmospheric pressure

TR 80043

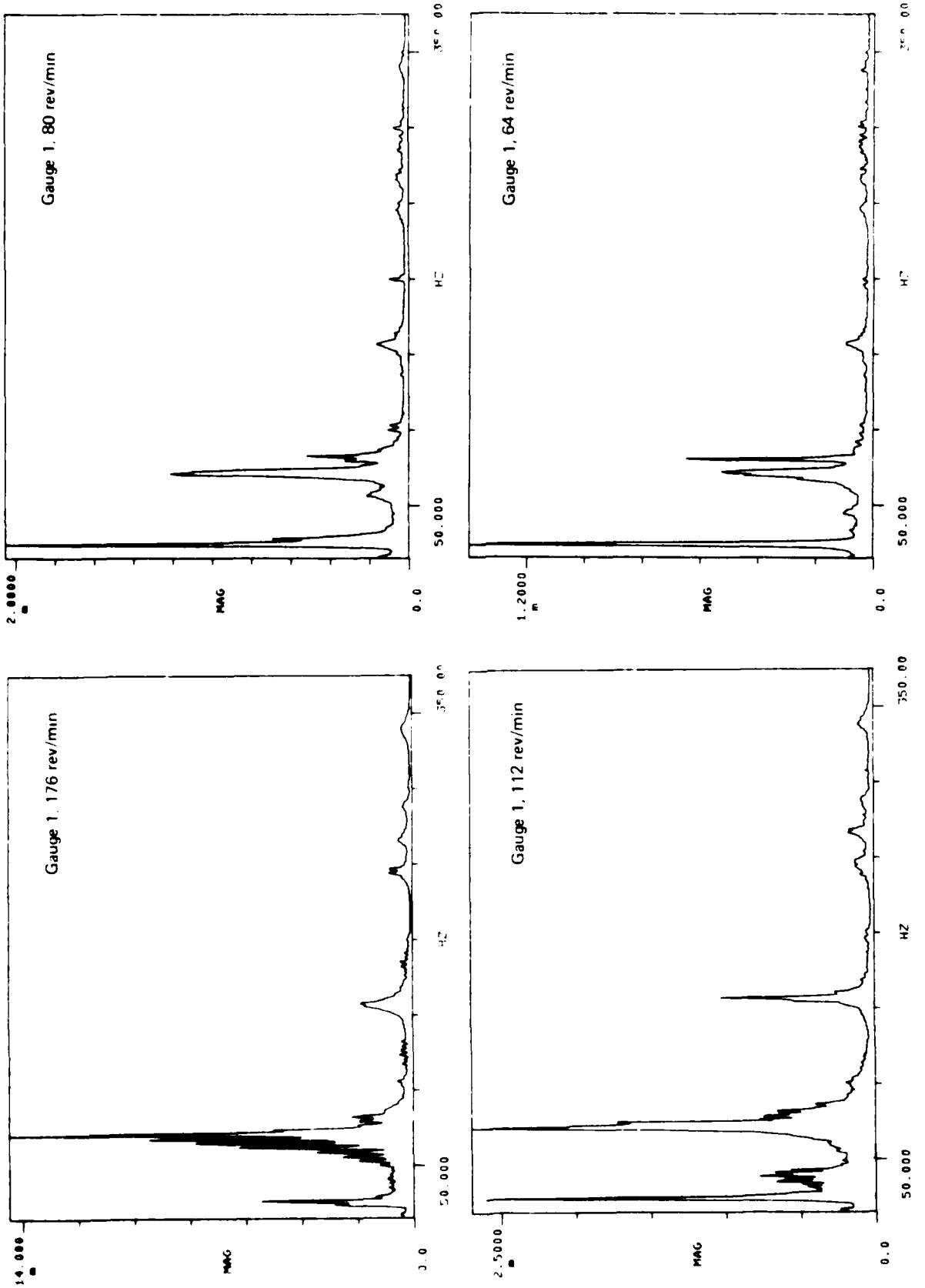

Fig 17b Blade response at selected fan speeds at atmospheric pressure

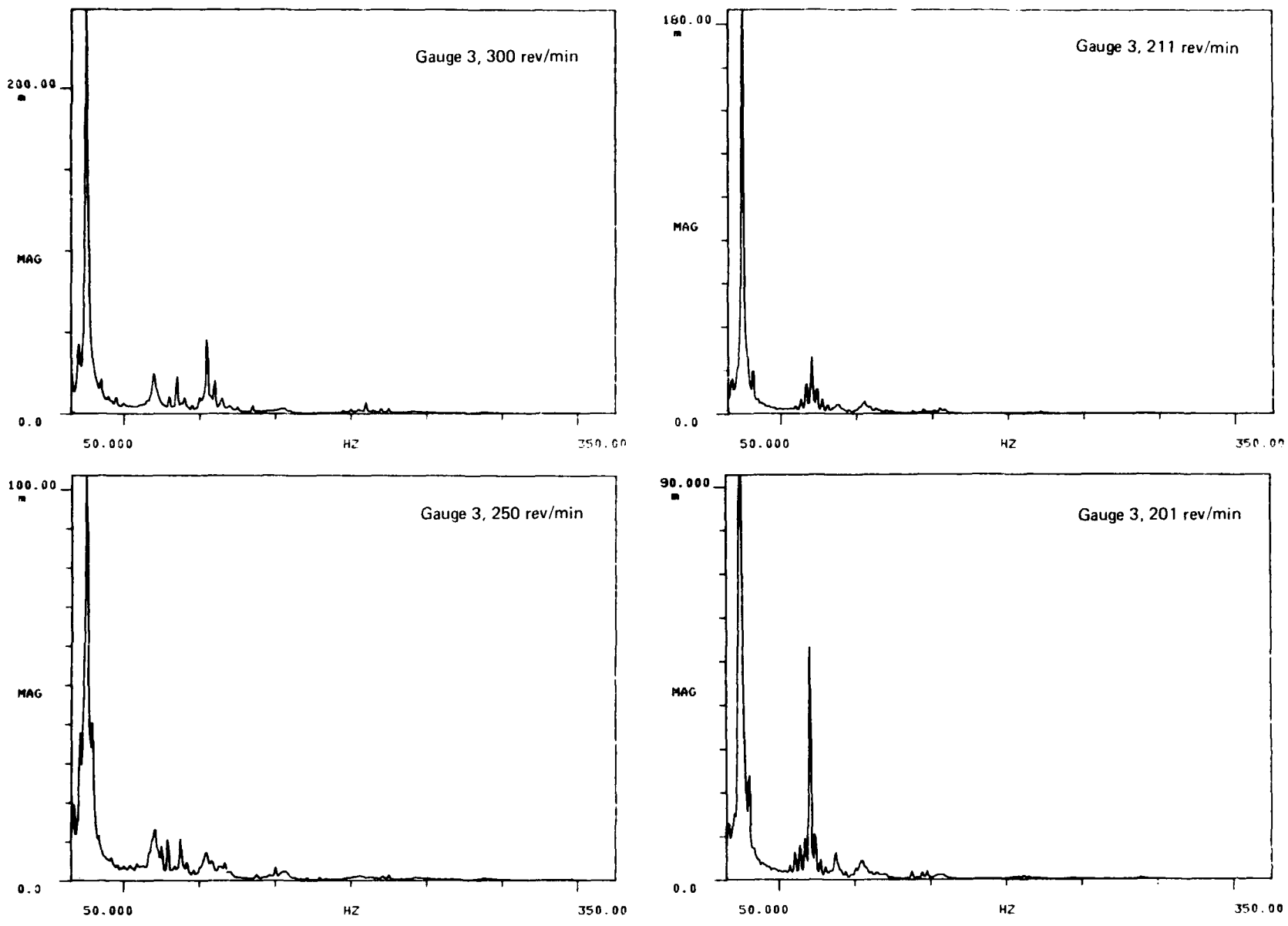

Fig 17c Blade response at selected fan speeds at atmospheric pressure

Fig 17c

TR 80043

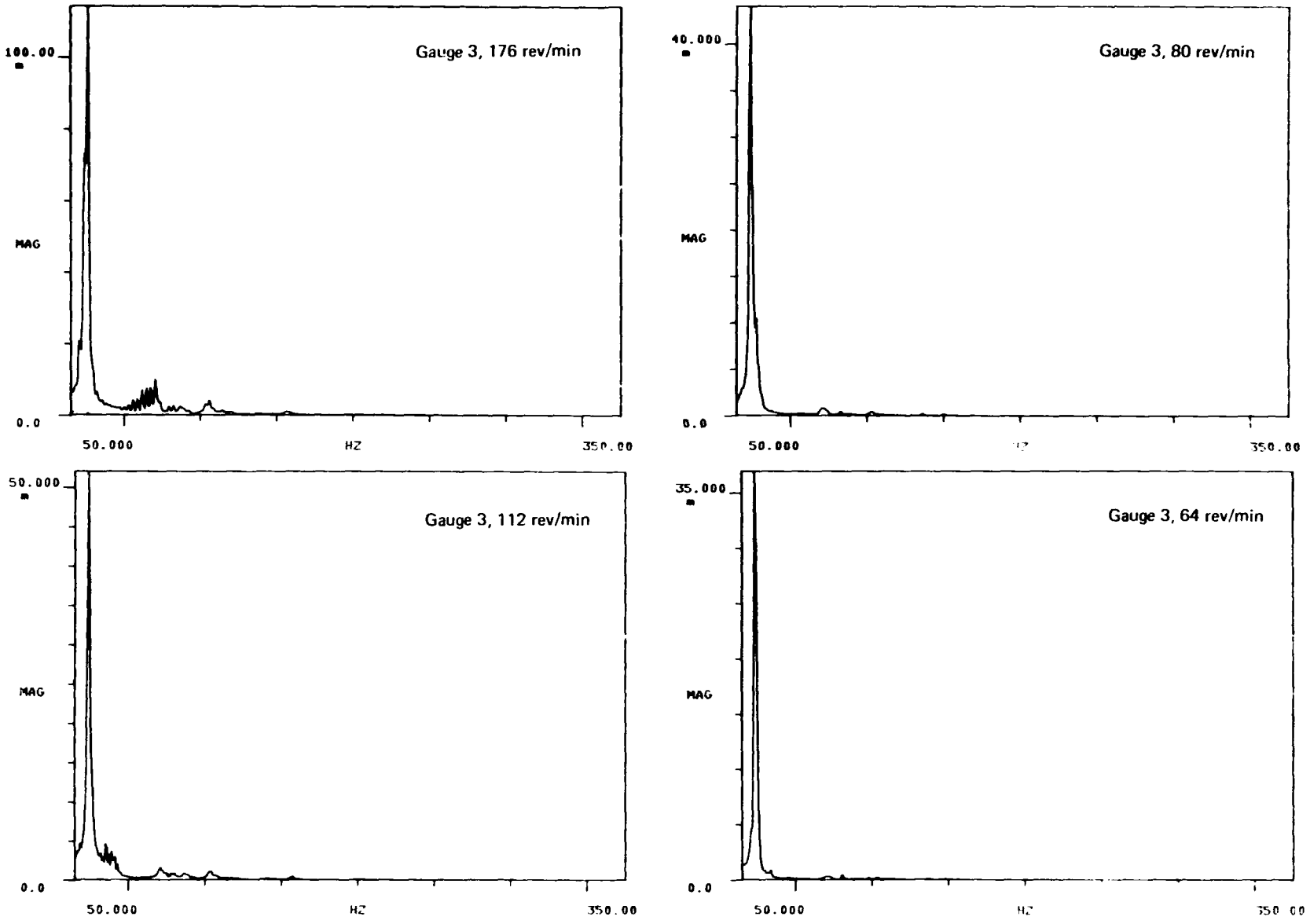

Fig 17d Blade response at selected fan speeds at atmospheric pressure

Fig 17d

Fig 18

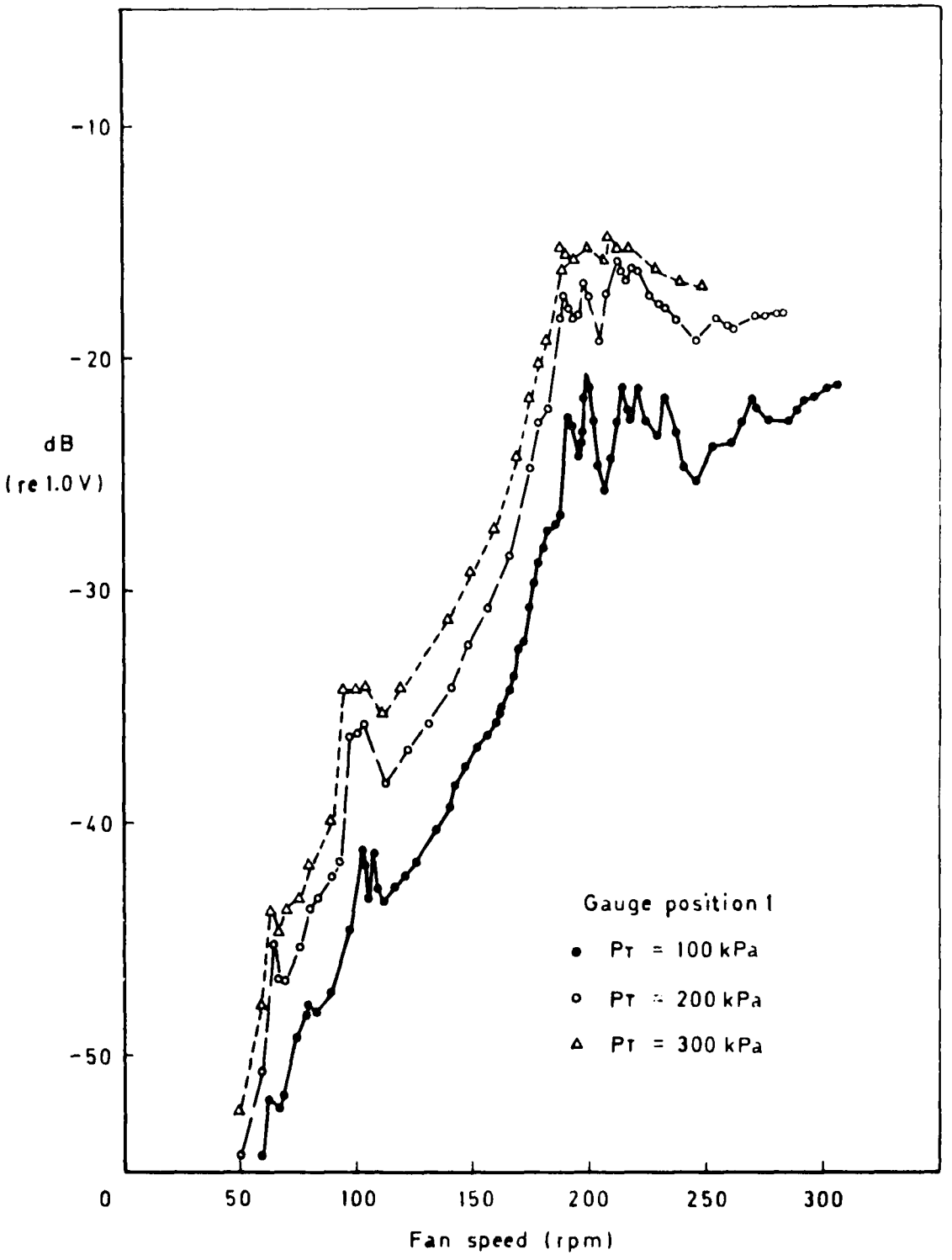

Fig 18 Effects of pressurisation. Gauge 1

TR 80043

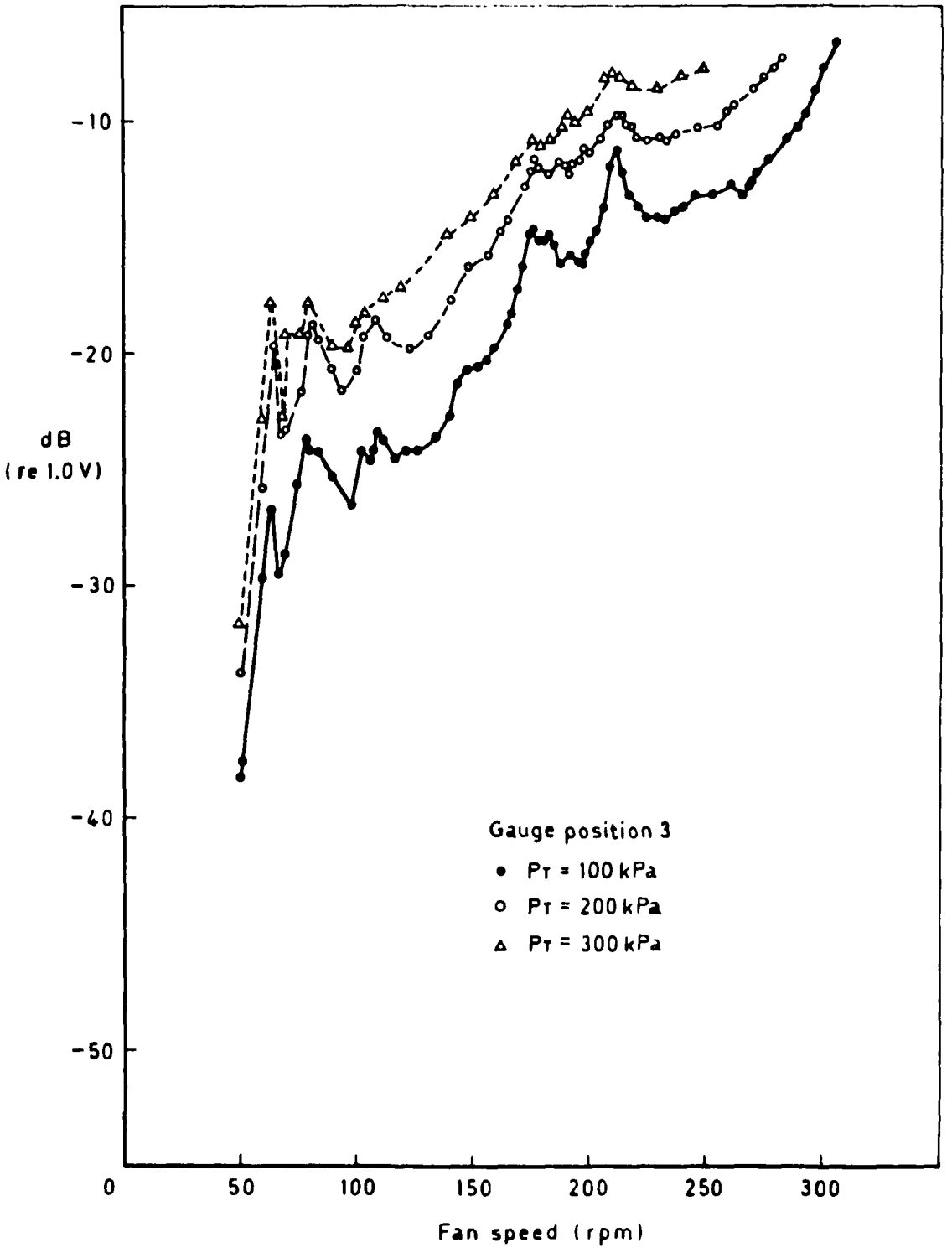

TR 80043

Fig 19 Effects of pressurisation. Gauge 3

Fig 20

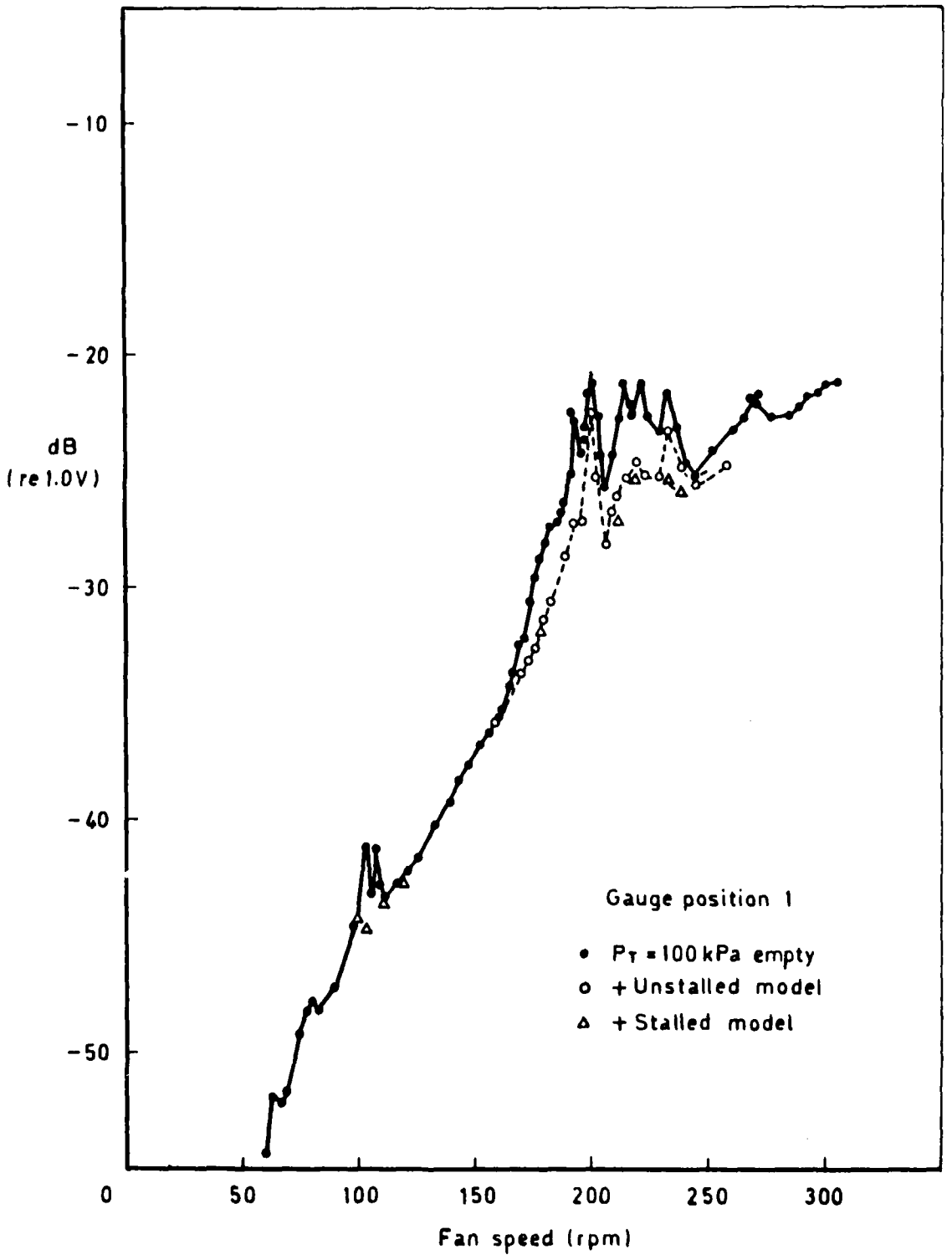

TR 80043

Fig 20 Effect of a model. Gauge 1

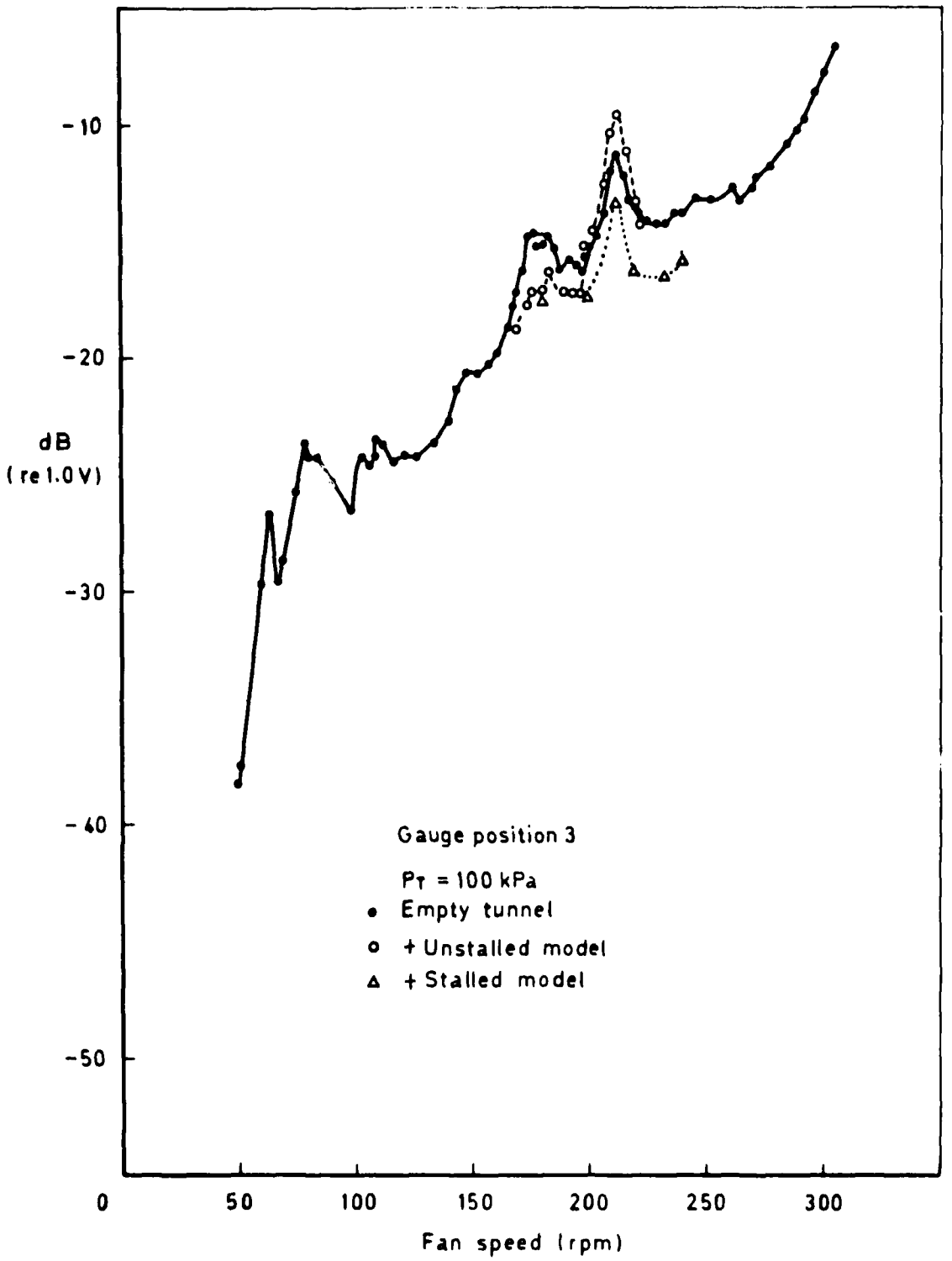

TR 8004.1

Fig 21 Effect of a model. Gauge 3

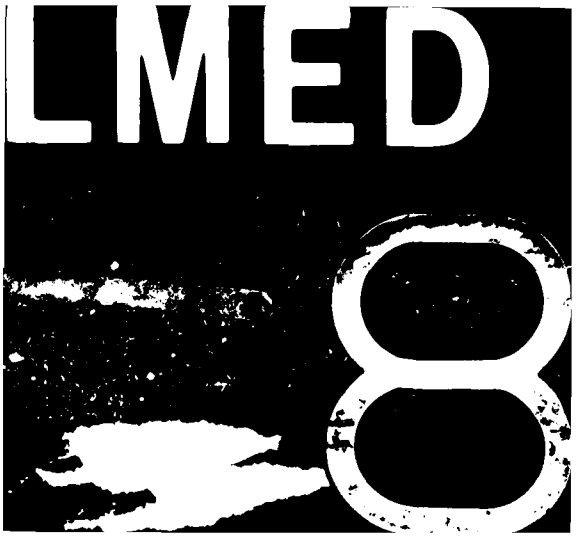
LMED
8